

MODELING OF SEISMIC SIGNATURES OF CARBONATE ROCK TYPES

A Thesis

by

BADR H. JAN

Submitted to the Office of Graduate Studies of
Texas A&M University
in partial fulfillment of the requirements for the degree of

MASTER OF SCIENCE

December 2009

Major Subject: Geophysics

MODELING OF SEISMIC SIGNATURE OF CARBONATE ROCK TYPES

A Thesis

by

BADR H. JAN

Submitted to the Office of Graduate Studies of
Texas A&M University
in partial fulfillment of the requirements for the degree of

MASTER OF SCIENCE

Approved by:

Chair of Committee,	Yuefeng Sun
Committee Members,	Mark E. Everett
	Walter B. Ayers
Head of Department,	Andreas Kronenberg

December 2009

Major Subject: Geophysics

ABSTRACT

Modeling of Seismic Signatures of Carbonate Rock Types. (December 2009)

Badr H. Jan, B.S., University of Tulsa

Chair of Advisory Committee: Dr. Yuefeng Sun

Carbonate reservoirs of different rock types have wide ranges of porosity and permeability, creating zones with different reservoir quality and flow properties. This research addresses how seismic technology can be used to identify different carbonate rock types for characterization of reservoir heterogeneity. I also investigated which seismic methods can help delineate thin high-permeability (super-k) layers that cause early water breakthroughs that severely reduce hydrocarbon recovery.

Based on data from a Middle East producing field, a typical geologic model is defined including seal, a thin fractured layer, grainstone and wackestone. Convolutional, finite difference, and fluid substitution modeling methods are used to understand the seismic signatures of carbonate rock types.

Results show that the seismic reflections from the seal/fractured-layer interface and the fractured-layer/grainstone interface cannot be resolved with conventional seismic data. However, seismic reflection amplitudes from interfaces between different carbonate rock types within the reservoir are strong enough to be identified on seismic data, compared with reflections from both the top and bottom interfaces of the reservoir. The seismic reflection amplitudes from the fractured-layer/grainstone and the

grainstone/wackestone interfaces are 17% and 23% of those from the seal/fractured-layer interface, respectively.

By using AVO analysis, it may be possible to predict the presence of the fractured layer. It is observed that seismic reflection amplitude resulting from the interference between the reflections from overburden/seal and seal/fractured-layer does not change with offset.

The thin super-k layer can also be identified using fluid substitution method and time-lapse seismic analysis. It shows that this layer has 5% increase in acoustic impedance after oil is fully replaced by injecting water in the layer. This causes 11% decrease and 87% increase in seismic reflection amplitudes from the seal/fractured-layer interface and the fractured-layer/grainstone interface after fluid substitution, respectively.

These results show that it is possible to predict carbonate rock types, including thin super-k layers, using their seismic signatures, when different seismic techniques are used together, such as synthetic wave modeling, AVO, and time-lapse analysis. In future work, the convolutional model, AVO analysis, and fluid substitution could be applied to real seismic data for field verification and production monitoring.

ACKNOWLEDGEMENTS

I would like to thank my committee chair, Dr. Sun, and my committee members, Dr. Everett, and Dr. Ayers, for their guidance and support throughout the course of this research.

Thanks also go to my friends and colleagues and the department faculty and staff for making my time at Texas A&M University a great experience.

Finally, thanks to my family for their encouragement, patience, and love during the completion of this research.

TABLE OF CONTENTS

		Page
ABSTRACT		iii
ACKNOWLEDGEMENTS		v
TABLE OF CONTENTS.....		vi
LIST OF FIGURES		viii
LIST OF TABLES.....		x
CHAPTER		
I	INTRODUCTION.....	1
	Previous Work	3
	Carbonate Reservoirs.....	4
	Carbonate Depositional Environments and Rock Types	7
	Porosity Classification	12
	Pore Types and Porosity Effect on Velocity	14
	Statement of the Problem.....	16
	Objectives.....	17
	Seismic Modeling of Carbonate Rock Types.....	17
	Thesis Structure.....	22
II	SEISMIC MODELING OF CARBONATE ROCK TYPES USING CONVOLUTIONAL MODEL	23
	Introduction	23
	Geological Model	24
	Method	26
	Results.....	28
	Conclusion.....	38
III	SEISMIC MODELING OF CARBONATE ROCK TYPES USING FINITE DIFFERENCE MODEL.....	40
	Introduction	40
	Method	41

CHAPTER	Page
Results.....	45
Conclusion.....	52
IV FLUID SUBSTITUTION.....	53
Introduction.....	53
Method.....	54
Results.....	55
Conclusion.....	61
V CONCLUSIONS.....	62
REFERENCES.....	64
VITA.....	67

LIST OF FIGURES

FIGURE	Page
1.1 Effect of grain size and sorting on porosity and permeability.....	5
1.2 The relationship between porosity and permeability in carbonate rocks...	6
1.3 Carbonate rock types based on Dunham classification.....	12
1.4 Ahr's integrated triangle diagram for genetic porosity types.....	14
1.5 P-velocity vs. porosity.....	15
1.6 Tuning effect with different bed thicknesses.....	18
1.7 Vertical resolution with different bed thicknesses.....	19
1.8 Lithologic model and seismic models at different frequencies.....	21
2.1 The geologic model used in this study.....	24
2.2 Convolutional modeling with 25Hz dominant frequency.....	31
2.3 Convolutional modeling with 50Hz dominant frequency.....	32
2.4 Convolutional modeling with 100Hz dominant frequency.....	33
2.5 Convolutional modeling using equal thickness for the layers with 25Hz dominant frequency.....	35
2.6 Convolutional modeling using equal thickness for the layers with 50Hz dominant frequency.....	36
2.7 Convolutional modeling using equal thickness for the layers with 100Hz dominant frequency.....	37
3.1 Shot records using FDM.....	45
3.2 Shot record using 50Hz based the original geologic model.....	46
3.3 Shot record using 100Hz based the original geologic model.....	47

FIGURE	Page
3.4 Comparison between the seismic signatures from convolutional model and finite difference model using 25Hz center frequency.....	48
3.5 Comparison between the seismic signatures from convolutional model and finite difference model using 50Hz center frequency.....	48
3.6 Comparison between the seismic signatures from convolutional model and finite difference model using 100Hz center frequency.....	49
3.7 Shot record with 25 Hz dominant frequency. The arrows show amplitude increase with increasing offset	51
4.1 Results of convolutional model before fluid substitution.....	56
4.2 Results of convolutional model after fluid substitution	57
4.3 Fluid substitution result	58
4.4 Finite difference model before fluid substitution with 25 Hz dominant frequency	59
4.5 Finite difference model after fluid substitution with 25 Hz dominant frequency	60
4.6 The difference between the before and after fluid substitution using the finite difference model	60

LIST OF TABLES

TABLE	Page
2.1 The physical properties for the geologic model used in this study.....	25
4.1 Rock properties for the fractured layer before and after fluid substitution...	55

CHAPTER I

INTRODUCTION

Carbonate reservoirs hold approximately 60% of the world's oil reserves, and 40% of the world's gas reserves. The Middle East has more than 60% of the world's oil reserves, and approximately 40% of the world's gas reserves. In the Middle East, 70% of the oil reserves and 90% of the gas reserves are held in carbonate reservoirs. The average recovery factor of carbonate reservoirs is only 35%. The recovery factor is lower in carbonate reservoirs than siliciclastics reservoirs due to the complex texture and pore network in carbonate rocks, and the heterogeneity of carbonate rocks in all scales. The largest oil field in the world, Ghawar, is in Saudi Arabia. This field is 280 km long and 25 km wide. It covers around 1.3 million acres, and it is a carbonate reservoir. Such giant fields still hold vast amount of hydrocarbons that cannot be extracted with conventional methods. Therefore, it should not be a surprise that carbonate reservoirs are key targets for technological and methodological advancements in oil and gas exploration and production (Schlumberger, 2007).

Carbonate reservoirs have high potential for field development. Nevertheless, the geology of these reservoirs is usually very complex, and rock properties change due to many factors such as depositional, diagenetic, and mechanical (fracturing) processes. These factors contribute to highly heterogeneous distributions of different permeability zones even within one carbonate reservoir. Generally carbonate reservoirs have porosity

ranging from 2% to over 30%. However, different carbonate rocks of different pore types and diagenesis can result in very different permeability, ranging from less than 1 millidarcy (md) to a few darcies (d). Furthermore, fracturing can create additional higher permeability from about a few d to tens of d. The complexity of carbonate rock types and fracturing creates a variety of zones that have very different reservoir qualities and flow properties. This presents great challenges for field development and production. Like many carbonate fields around the world, the Ghawar field exhibits reservoir anomalies and production problems such as early water breakthrough. It is found that thin layers of extremely high permeability called “super-k layers” cause severe water breakthrough in the field. The presence of super-k layers causes complicated fluid movement, and results in bypassed oil and low recovery. Understanding the distribution of these layers can improve field development and help to maximize hydrocarbon recovery.

Seismic data have been extensively used in past decades for imaging the structures of sedimentary basins and hydrocarbon reservoirs. With improved technology we use seismic data to predict reservoir rock properties. However, low seismic resolution is still a concern for mapping the fine-scale reservoir heterogeneity that is needed to characterize sub-meter-scale fluid flow and its relationship to field production. We can directly relate the geology to seismic data where cores and logs are available. Seismic data of appropriate resolutions offer the possibilities of characterizing reservoir heterogeneity in the inter-well regions. Seismic modeling may be the best technique to explore the relationships between rock and fluid properties and seismic response. Thus,

seismic technology should be further investigated and utilized for advanced carbonate reservoir characterization, along with enhancement of hydrocarbon recovery.

In the following, I will briefly review some previous work relevant to this study, and summarize basic background in carbonate geology (Ahr, 2008) and carbonate geophysics (Palaz and Marfurt, 1997). Then I will present my thesis objectives, methods and thesis outline.

Previous Work

Understanding the heterogeneity of carbonate reservoirs can help to overcome the challenges associated with their exploration and development. Many studies have been attempted to understand the effects of rock properties on seismic data and to characterize the geology of the subsurface away from wells.

Anselmetti and Eberli (1993), Sun (2004) and Sayers and Latimer (2008) discussed the effect of porosity on seismic velocities and the contribution of the pore shape on the relationship between porosity and seismic velocity. Wagner (1997) studied the effect of carbonate diagenesis on seismic data and showed how 4-D seismic data can detect diagenesis of carbonate rocks. Dasgupta et al. (2001) showed that integrating petrophysical information with 3-D seismic data with reservoir simulation improves porosity mapping in the Khuff-C reservoir. Amplitude inversion of 3-D seismic data helped to reveal the tight zones in the reservoir.

Few studies have been attempted to identify carbonate rock types within a reservoir using seismic methods. In this study I investigate the seismic signature of carbonate rock types at the wellbore and correlate it with seismic data away from the well. The aim is to predict the high permeability zones within the reservoir, which will help improve hydrocarbon recovery.

Carbonate Reservoirs

Carbonates are sedimentary rocks deposited typically in warm shallow waters. Unlike siliciclastics, carbonate rocks are biogenic in origin. They mainly consist of calcium carbonate and some fragments of algae, coral, skeletal remains and other marine sediments. Unlike clastic rocks, carbonate rocks are deposited locally where grains are deposited close to where sediments are created. This local deposition contributes significantly to the heterogeneity of carbonate rocks. Although carbonates are composed of simple mixtures of dolomite, calcite, and aragonite, heterogeneity due to fabric, texture, porosity, cementation, and fractures leads to a high variability of carbonate rock properties. After deposition, ranges of physical and chemical processes occur that alter the rock structure and change the porosity and permeability.

Grain size and sorting are important attributes in studying carbonates because of their influence on porosity and permeability. Large grains have big pores with wide pore throats that enhance permeability. Sorting has a large effect on both porosity and permeability because sorting affects the geometry between the pores and pore throats.

The pore-pore throat relationship has a larger effect on permeability than does pore geometry. Figure 1.1 is based on a sand experiment, and shows the grain size and sorting effects on porosity and permeability.

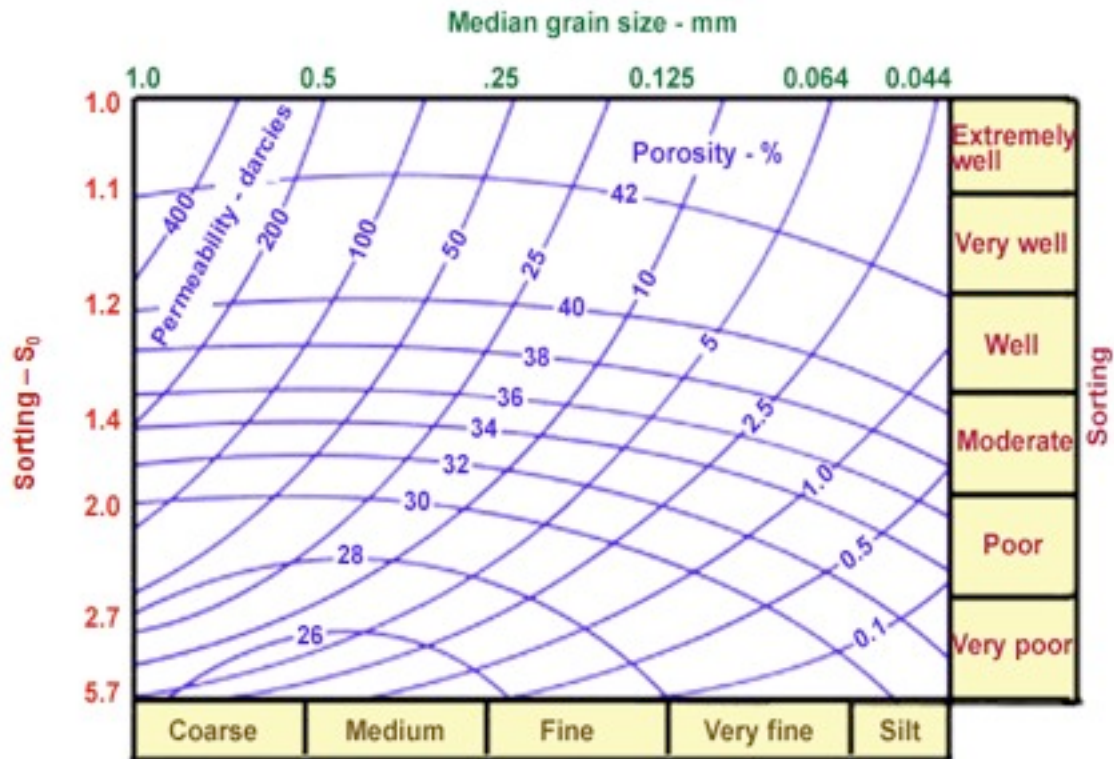


Figure 1.1. Effect of grain size and sorting on porosity and permeability (Ahr, 2008).

The relationship between porosity and permeability for a variety of carbonate rocks found in typical reservoir formations is shown in Figure 1.2. For a given porosity value there exists a wide range of permeability values caused by the presence of different carbonate rock types. For example, if a 20% porosity value is chosen, the corresponding permeability values range from 3 md to more than 3 d. Permeability values for a reservoir can be scaled as follows (North, 1985):

- Poor to fair <math><0.001-0.015\text{ d}</math>
- Moderate $0.015-0.05\text{ d}$
- Good $0.05-0.25\text{ d}$
- Very good $0.25-1\text{ d}$
- Excellent $>1\text{ d}$

Based on this, for 20% porosity value, we can have moderate, good, and very good reservoir permeability scales in the carbonate reservoir shown in Figure 1.2. This non-uniqueness in the porosity-permeability relationship reflects the level of complexity in carbonate reservoirs and how different carbonate rocks affect the porosity and permeability differently.

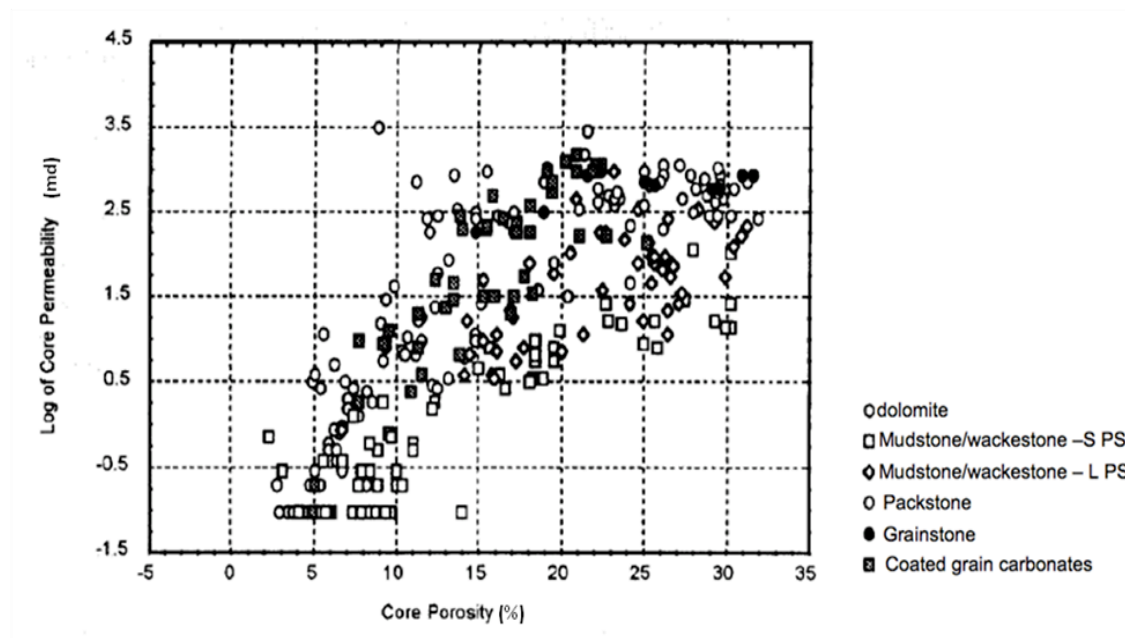


Figure 1.2. The relationship between porosity and permeability in carbonate rocks (Davis and Fontanilla, 1997).

Carbonate Depositional Environments and Rock Types

Most carbonate rocks originate in marine environments, which are divided into smaller subenvironments characterized by rock properties. Oceanographic studies show that carbonate platforms can be either ramps where the slope of the platform does not have any pronounced break, or shelves where platform slope have a major break. There are six depositional environments associated with carbonate ramps and shelves:

1. Beach
2. Tidal-flat and lagoon
3. Shallow subtidal
4. Slope-break
5. Slope
6. Basin

Each environment has its unique characteristics. Predicting the location of each environment will enable us to locate the corresponding lateral succession.

Beaches are found at the boundary between land and sea. They are attached directly to the sea if they are extended from the land, and detached if they are separated from the land by lagoons or barrier islands. The beach environment is further divided into three divisions: lower, middle, and upper shorefaces. The characteristics of these shorefaces depend mainly on the behavior of the incoming ocean waves. The lower shoreface is controlled by oscillatory waves. The middle shoreface is controlled by the unidirectional currents. The upper shoreface indicates the breaking waves zone, where

the beach-face beds are formed. Beach environments are generally very well sorted and considered to have the highest porosity among other depositional environments.

A tidal-flat environment is protected from ocean waves, which causes this environment to become mud-dominated. Fenestral porosity, irregular cavities in carbonate sediments shaped like birdseye, is common and is generally formed by algal mat decomposition. The tidal-flat environment can be divided into three zones:

1. The subtidal zone: the open ocean or lagoonal area (always wet)
2. The intertidal zone: the channel areas between land and water (moderately wet)
3. The supratidal zone: the area above high tide (typically dry)

The subtidal zone sediment properties vary depending on the climate and water exchange between open sea and the lagoon. A dry climate may result in the formation of evaporite deposits and some lime-mud accumulation. A wet climate will decrease the amount of evaporite deposits and increase lime-mud accumulation.

The intertidal zone sediment properties depend on the current to move the water from the subtidal to the supratidal zone. When the water is dried or drained off, the mud accumulation can build in progradational sequence.

The supratidal zone is almost a dry zone but sometimes flooding can occur as a result of storms and heavy rains. Wetting and drying cycles can cause mud cracks, stromatolites, and fenestral pores in the lower supratidal zone. With storms and tides eroding the cracked surfaces, flat pebbles are created. These flat pebbles, along with fossils are the main grain types in tidal-flat environments. Diagenetic processes usually generate reservoir porosity in tidal-flats.

The shallow subtidal environment is the region located from the low tide line to water depth ~200m. Unlike the tidal-flat environment, the shallow subtidal environment sedimentary characteristics vary significantly depending on several factors:

1. bathymetry
2. hydrology
3. carbonate production
4. taxonomic variety

Usually the seabed bathymetry is monotonous and does not support accumulation of grainy sediments. Bathymetric features such as patch reefs may collect some grainy facies around and on topographic highs. The patch reefs with the associated grainy sediments located on bathymetric highs have high tendency to become commercial reservoirs since they are characterized by high value of depositional porosity.

Slope-break environments have high carbonate production because the seabed is located within the nutrient-rich, oxygenated, photic zone. Unlike distally steepened ramps, open and rimmed shelves facies change at slope break. Distally steepened ramps are located at depths below the base of fair-weather waves that interact with sedimentation. High-energy sediments are usually located on the seaward side of the slope break, while the low energy sediments build up on the leeward side. This sorting helps to identify the polarity of the environment. Slope break sediments show three different kinds of depositional porosity:

1. Intergranular: the space between sediment grains
2. Intraframe: the space within the whole skeletal material

3. Intraparticle: the voids inside the skeletal material

The intergranular porosity can provide the highest permeability to the reservoir, but may also expose the reservoir to the high risk of cementation caused by diagenesis. The other two kinds of porosity have less connectivity between pores, which act as separate vugs.

Slope facies can indicate slope characteristics, environmental processes, and proximity to the overlying slope break. Depending on slope steepness, sediments typically accumulate around the base of the slope. Facies found in the deposits toward the basin in general include debris fans, slumps, and turbidities. Interparticle porosity at the base of the slope is usually low because of the fine matrix.

The last depositional environment associated with shelves and ramps is the basin. The depth of the basin and the facies associated with the basin environment vary. There is no distinctive depth or a specific description for basin facies. In order for carbonate sediments to accumulate in the basin, the depth of the water should be shallower than the “carbonate compensation depth” otherwise carbonates will dissolve. Basin sediments typically include both carbonate materials and siliciclastics. Usually the facies are dark color, fine-grained, organically rich, and thin bedded.

Beach environments may or may not include dunes depending on the supply of sediments. Lagoon environments may include poorly sorted washover deposits and some coarse deposits from the beach environment. Shallow subtidals generally contain mudstones and wackestones. The slope break environments typically contain skeletal reefs with layers of grainstones. Successions of slope top environments include

turbidities and debrites. The basin environment commonly contains distal turbidites with rhythmites and laminites. These are the ideal depositional successions on carbonate ramps and shelves.

Archie (1952) made the first tentative step in relating rock fabric to petrographical rock properties in carbonate reservoirs. Archie focused on estimating porosity and permeability based on capillary pressure measurements.

The Dunham classification (1962) of carbonate rocks is widely used by oil companies (Figure 1.3). It is based on depositional texture and composition according to the texture and grain size of the rocks. The Dunham classification is similar to the Folk classification (1959), which details the relative proportion of allochems, grains that form limestone's framework, in the rock and describes the type of matrix if one is present. The Folk classification uses suffixes to describe the matrix, and prefixes to describe the main (non-matrix) component.

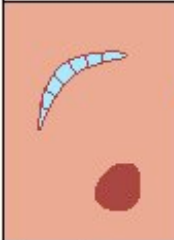
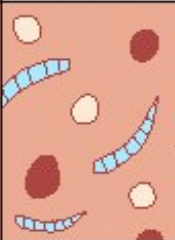


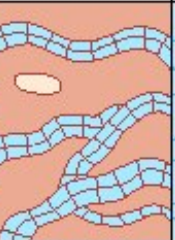

Mudstone	Wackestone	Packstone	Grainstone	Boundstone	Crystalline
					
Less than 10% grains	More than 10% grains	Grain-supported	Lacks mud and is grain-supported	Original components were bound together	Depositional texture not recognizable
Mud-supported					
Contains mud, clay and fine silt-size carbonate					
Original components not bound together during deposition					
Depositional texture recognizable					

Figure 1.3. Carbonate rock types based on Dunham classification (Schlumberger, 2009).

Unlike siliciclastics, carbonate deposits generally tend to accumulate on local bathymetric highs. Knowing the general sedimentological processes associated with carbonate environments greatly helps in determining the rock types expected to be found in the reservoir. In order to determine the origin of a carbonate reservoir, the various porosity types of the reservoir rocks must be identified.

Porosity Classification

Many studies have been performed to classify and understand the different porosity types in carbonate reservoirs. A recent study by Ahr (2008) classified porosity in carbonate rocks into three end members: depositional, fracture, and diagenetic. When

more than one mechanism affects the pore system, a hybrid pore system exists (Figure 1.4). This classification takes into account the petrophysical properties to determine the reservoir quality.

Diagenesis is one of the processes that affect porosity in carbonate rocks. It alters the porosity by physical mechanisms such as replacement, recrystallization, dissolution, compaction, and cementation. Diagenetic processes may be mechanical, chemical, biological, or combinations of more than one. An example is the reduction in volume by compaction, which may change grain packing. Mechanical diagenesis has a strong influence on the porosity of carbonate rocks. However, chemical diagenesis is considered the most important change mechanism in carbonate reservoirs. Replacement, recrystallization, cementation, and dissolution are chemical diagenesis processes. Replacement completely changes one mineral into another. An example is dolomite replacing calcite and aragonite. Recrystallization changes the crystal morphology without changing the mineral composition. Cementation fills pores and joins loose grains. For example, calcite might crystallize either as flat rhombohedra or as dogtooth spar depending on the environmental conditions. Dissolution takes place when the rock-water system is not at equilibrium. Dissolution may create karst or large pores as vugs or molds. Biological diagenesis takes place in the form of bioerosion, grinding, or as a result of plants and animals eroding the rock surface. The impact of bioerosion on carbonate reservoirs porosity is generally minor. Overall, variations in porosity types can produce complex fluid pathways that will generally decrease well performance.

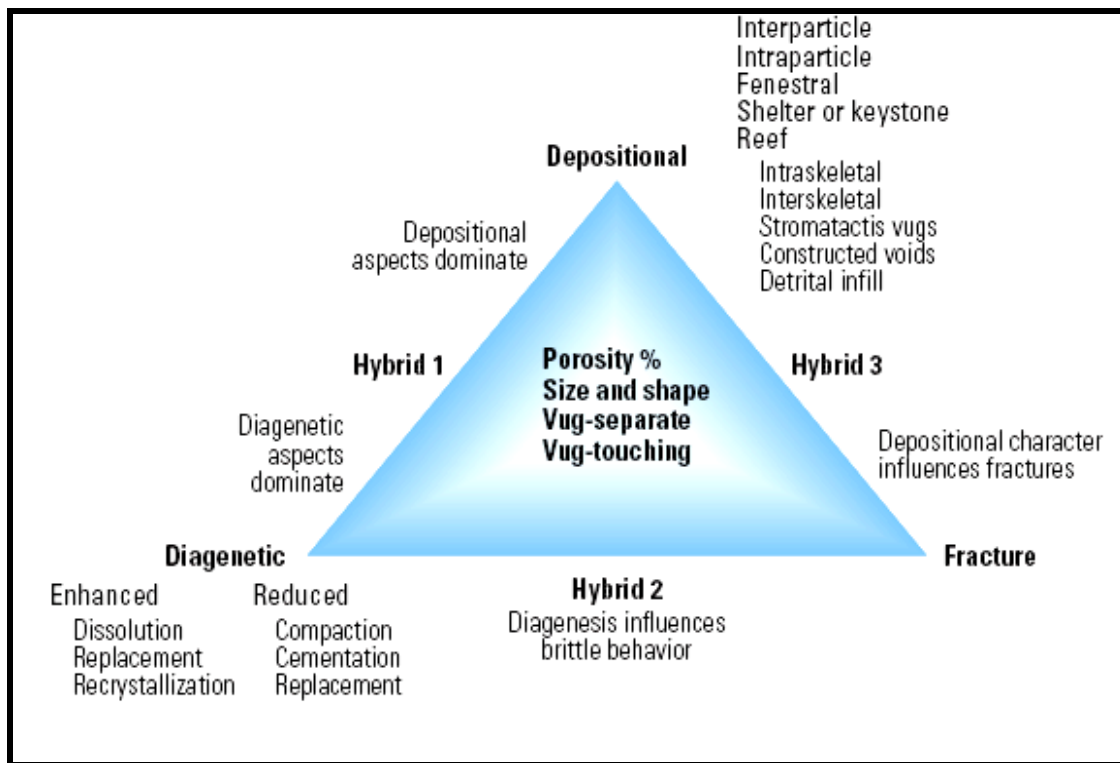


Figure 1.4. Ahr's integrated triangle diagram for genetic porosity types (Ahr, 2008).

Pore Types and Porosity Effect on Velocity

The heterogeneity of carbonate rocks is expected to have strong influence on acoustic and seismic wave propagation. Several studies have related the effects of pore shape and porosity on the velocity of seismic waves in carbonate rocks (Anselmetti and Eberli, 1993). These studies show the significance of pore structure on elastic wave propagation. Under certain conditions the effect of pore shape is greater than the effect of porosity on seismic velocity. For example, the compressional wave (P-wave) velocity difference in two limestone rocks with the same porosity can be as large as 2.5 km/s (Sun, 2004).

Carbonate rocks have complex porosity types, such as molds, intraparticle, interparticle, intercrystalline, fractures, fenestral and vugs. Porosity types affect both hydrocarbon migration and seismic properties such as velocity. Generally an inverse relationship exists between velocity and porosity as shown in the Figure 1.5. However, we notice that the data points are scattered possibly due to variations in pore geometry.

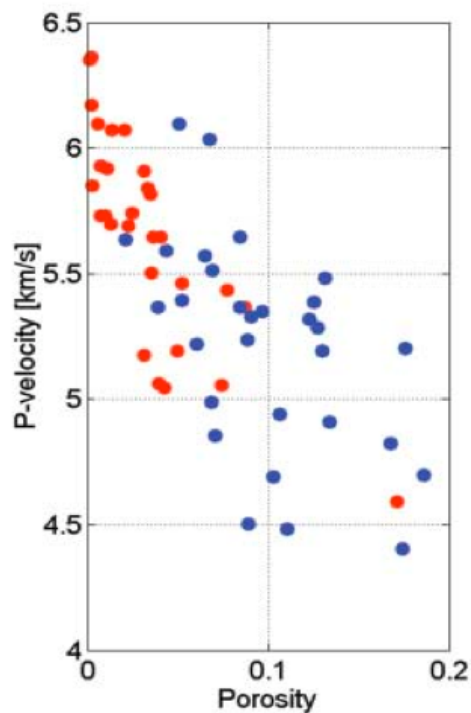


Figure 1.5. P-velocity vs. porosity. Red dots represent air-saturated limestone. Blue dots represent air-saturated dolomite. (Sayers and Latimer, 2008).

Seismic velocity is a measure of the compressibility and rigidity of the rock. Seismic velocity is low in rocks containing thin pores that are easily deformed. Seismic velocity is high in rocks containing spherical voids and cavities that are difficult to deform.

Intercrystalline porosity implies that the spaces between particles are of roughly the same size. Interparticle porosity refers to pores that have a non-uniform size distribution of any size. Rocks with intercrystalline and interparticle porosity generally have low seismic velocity as they are easily compressed by overburden pressure. Moldic porosity is formed when shells dissolve thereby creating a void space. Moldic, vuggy and intraparticle porosities have high velocity because the pores are not easy to deform. Fenestral porosity refers to irregular cavities within carbonate rocks formed by burrowing animals or plant roots. Rocks with fenestral porosity tend to have low seismic velocity and easy to deform as pressure increases, causing seismic velocity to increase.

The seismic velocity of a fractured carbonate rocks depends on the fracture orientation and elastic wave polarization. In general, a P-wave has much lower velocity in a highly fractured rock than in a non-fractured one. Both P-wave and shear wave (S-wave) propagation is faster in directions parallel to the fractures than perpendicular to the fractures (Wang, 1997). There may also have a shear wave splitting phenomenon in fractured rocks (Crampin and Peacock, 2008).

Statement of the Problem

My thesis research is to perform preliminary investigation on whether seismic method can be used to identify different carbonate rock types within reservoirs. Especially I will study how seismic methods can be helpful in delineating the thin super-k layers, which causes water breakthroughs and subsequently hinder field production.

Objectives

To address the scientific problems identified above for this research, I have investigated the seismic methods used in hydrocarbon exploration and production that could help identify different carbonate rock types within a carbonate reservoir. Their seismic signatures are analyzed within the limit of seismic resolution. The second objective of this research is to understand the seismic response of thin super-k layers through model investigation and numerical simulation. I have identified and recommended seismic methods that could be used to characterize the super-k layers, and the fluid changes that occur in these layers during production.

Seismic Modeling of Carbonate Rock Types

Seismic method is used in this study to identify different carbonate rock types. Seismic data does not record rock properties; it records reflected acoustic waves from the subsurface layers. Generally seismic data have been used to identify structural traps for potential hydrocarbon. With the improvement in seismic data quality we should be able to detect thin carbonate layers, which are below conventional seismic resolution.

There are a couple of factors in seismic data that we have to consider. One is the acoustic impedance contrast between the targeted reservoir rocks and the layers above and below. The acoustic impedance depends on the velocity and density of rocks. Another two factors are the seismic wavelength (λ) and the thickness (d) of the target

interval. The rule is that the reservoir thickness (d) should be at least one quarter of the wavelength (λ) of the seismic wave in order for that layer to be visible on seismic data (Liner, 1999).

$$d = \frac{\lambda}{4} \quad (1.1)$$

In the figure below the two traces on the left are the top and bottom reflections and they have the opposite polarity. The third trace on the right is the summed trace showing how it would appear in the migrated data. The tuning occurs when the sum of the top and bottom amplitudes is at maximum and that is when the bed thickness is one quarter of the wavelength.

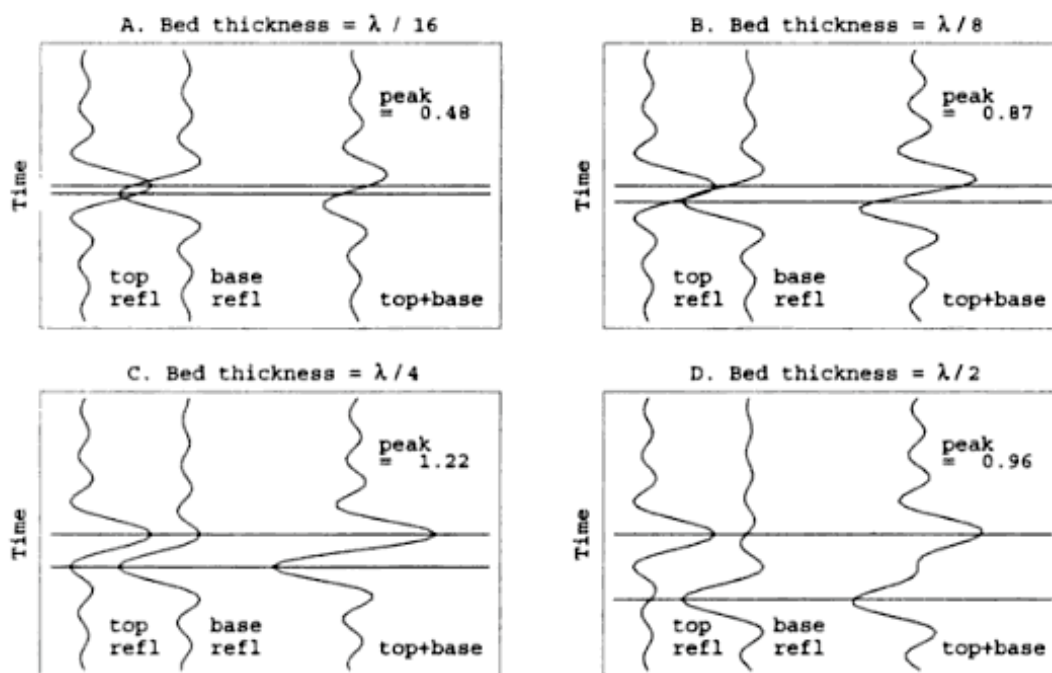


Figure 1.6. Tuning effect with different bed thicknesses (Liner, 2004).

The vertical resolution is another factor that is important in the case of thin beds. Figure 1.7 shows reflections from the top and bottom boundaries of a thin bed having the same polarity. When bed thickness is one quarter of wavelength we start to see two peaks on the summed trace. However, if the bed thickness is less than one quarter of the wavelength, we will not be able to distinguish the peaks of the top reflection from the bottom one.

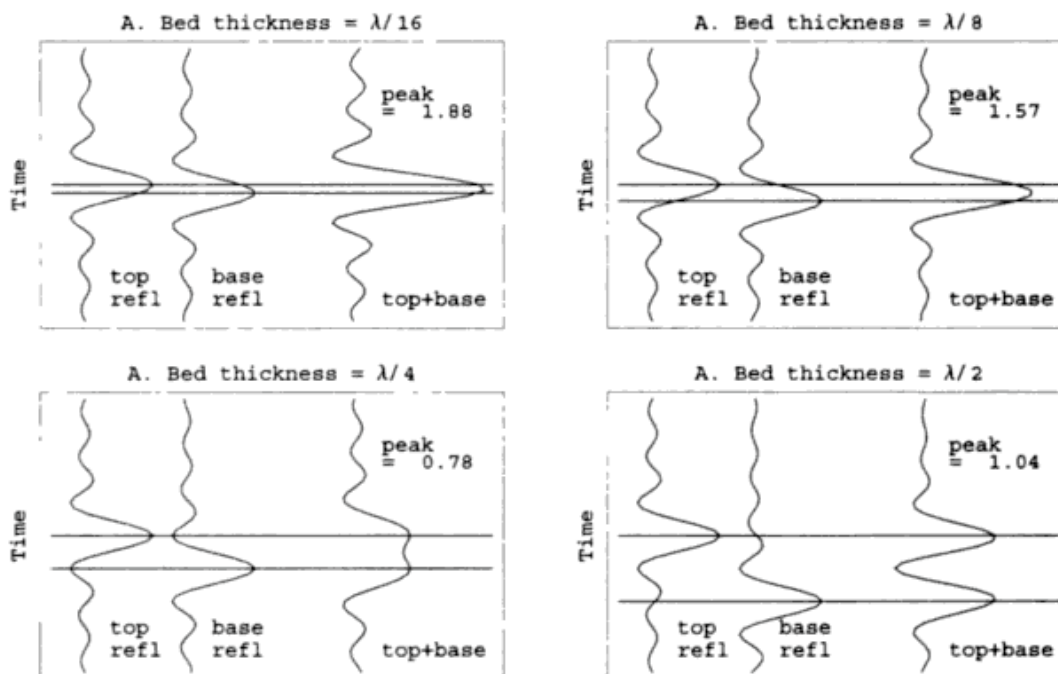


Figure 1.7. Vertical resolution with different bed thicknesses (Liner, 2004).

The velocity in carbonate rocks is usually faster than in siliciclastics, so that for a given frequency the wavelength is longer in carbonate rocks, which further decreases seismic resolution. Usually the top of a carbonate layer, overlain by siliciclastics with a lower velocity, is easy to distinguish on a seismic section. However, if the target is embedded in carbonate layers it is not easy to visualize due to the low acoustic impedance contrast between the carbonate layers.

In carbonate reservoirs, beddings formed over platform flanks may appear in seismic section as unconformities but they are caused by lateral facies change. Pseudounconformities have a tendency to form at the margins of platforms and reefs due to the nature of carbonates where sediments form locally and mix with muds on the edge of the buildup. This will result in change of bed thickness. In seismic sections this may appear as onlap or downlap patterns following facies change where they should be following bedding surfaces. Having higher frequency data may increase the limit of seismic resolution and thin beds would be distinguishable. From Figure 1.8, we can see that at 25Hz the interfingering of beds shows onlap features. At higher frequencies the interfingering zone is resolved and shown as echelon lens shaped reflectors (Wolfgang, 1999).

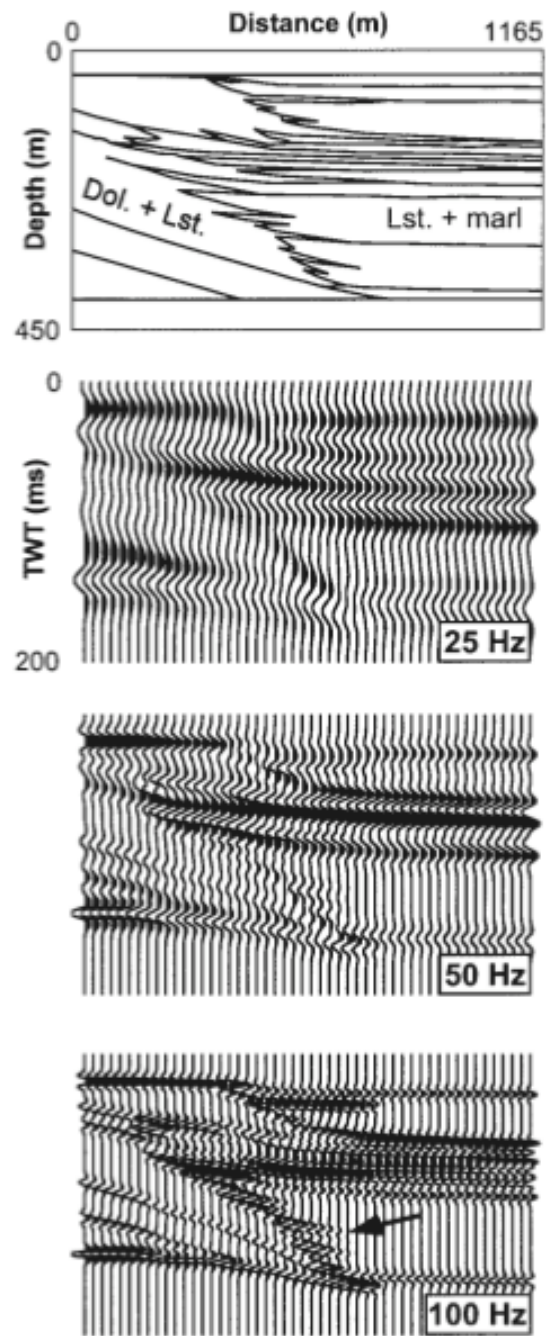


Figure 1.8. Lithologic model and seismic models at different frequencies (Bracco Gartner and Schlager, 1999).

Thesis Structure

In this study I investigate three seismic modeling methods to study the seismic signatures of different carbonate rock types, namely, convolutional modeling, finite difference modeling, and fluid substitution modeling. These methods would help identifying the seismic signatures of carbonate rock types.

In this chapter, I introduced some geological and geophysical backgrounds about carbonate reservoirs and the challenges that we have encountered.

In Chapter II, I will discuss the first modeling method in this study, which is the convolutional model. The synthetic seismograms calculated using this model are used to correlate the seismic signatures to the different carbonate rock types. This model represents the seismic signatures at the well location.

The finite difference model is addressed in Chapter III. This model includes seismic signatures away from wells. The seismic signatures from this model are compared to the seismic signatures from the convolutional model to be correlated to the lithology.

In Chapter IV, I will investigate fluid substitution technique for its feasibility to identify the super-k layers and the fluid flow movement in thin layers.

CHAPTER II

SEISMIC MODELING OF CARBONATE ROCK TYPES USING CONVOLUTIONAL MODEL

Introduction

In this chapter, I use the convolutional model to generate synthetic seismic data in order to study the seismic signatures of carbonate rock types. The main purpose of using the convolution model is to have a simple model to relate the seismic signature to the geology. In the convolution model, only primary waves (V_p) are calculated. In other words, there are no converted or shear waves (V_s) to be included. This model can be considered the perfect result of data processing because the end result does not have any noise or multiples or converted waves. And the reflections show their true amplitude and they are in the correct position.

The only direct way to relate the seismic data to the geology is by core and log data, which gives us information about the geology at the well location only. Seismic data is the only method we can use to predict the geology away from wells. If we can tie the information we have at the well location with the seismic data away from the well, we can have better prediction of the geology away from the well.

In this study, I use core and log data to construct the geological model at the well location and generate the synthetic seismic data to find the signatures of carbonate rock

types. The seismic signatures so defined could be correlated to other wells and in between the wells.

Geological Model

The original field data used in this study is from a producing carbonate field in the Middle East. Based on field core and log data, a geologic model from this producing carbonate reservoir is developed as shown in Figure 2.1. The top layer of the reservoir in the geologic model is fractured. This layer can cause unexpected fluid flow movement in the reservoir or water breakthrough. Identifying the seismic signature of this fractured layer would improve field development significantly.

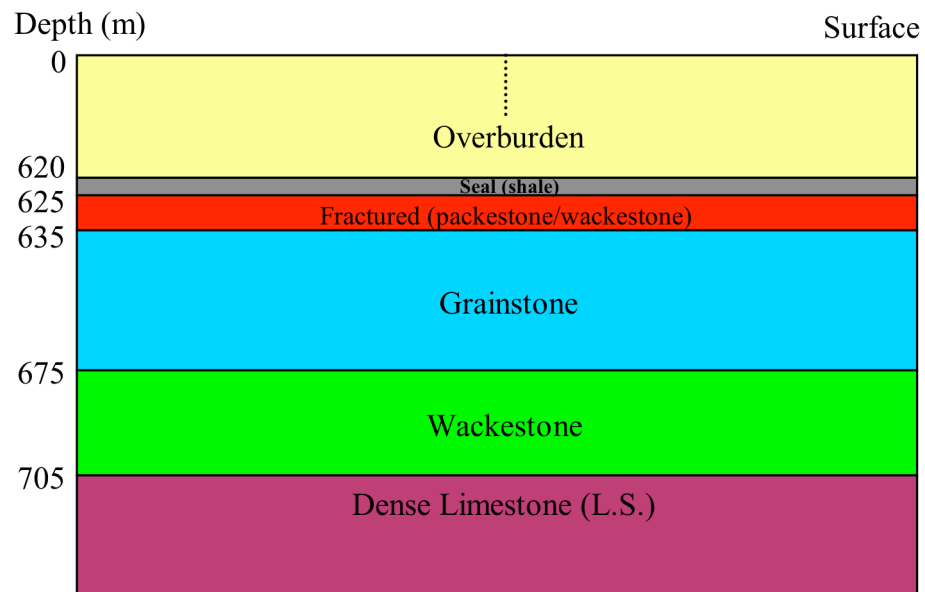


Figure 2.1. The geologic model used in this study.

The parameters for the layers above the seal are averaged out for simplicity. The thickness of the reservoir is 80 meters consisting of a fractured layer at the top, grainstone, wackestone, and a dense limestone at the bottom. The depth, compressional and shear velocities, density, porosity, acoustic impedance, and reflection coefficient for each layer are shown in Table 2.1.

The reflection coefficient (RC) of the fractured-layer/seal interface is equal to -0.19. Physically this means that the acoustic impedance (AI) of this layer is lower than the seal layer above approximately by 38%. The grainstone/fractured layer interface has reflection coefficient equal to -0.03, which means that the acoustic impedance of the grainstone is lower than the fractured layer above roughly by 6%. The reflection coefficient of the wackestone/grainstone interface is equal to 0.04, which means that the wackestone layer has higher acoustic impedance than the grainstone layer above by about 8%.

Table 2.1. The physical properties for the geologic model used in this study.

<i>Lithology</i>	<i>Depth</i> (<i>m</i>)	<i>V_p</i> (<i>m/s</i>)	<i>V_s</i> (<i>m/s</i>)	<i>Density</i> (<i>g/cc</i>)	<i>Porosity</i>	<i>AI</i>	<i>RC</i>
<i>Non reservoir</i>	0	3625	1694	2400	0.184	8.70	n/a
<i>Seal</i>	620	5203	2681	2680	0.018	13.94	0.23
<i>Fractured carbonate</i>	625	3785	1924	2500	0.127	9.46	-0.19
<i>Grainstone</i>	635	3835	1935	2310	0.241	8.86	-0.03
<i>Wackestone</i>	675	4066	2047	2380	0.199	9.68	0.04
<i>Dense limestone</i>	705	4950	2607	2550	0.096	12.62	0.13

Method

Using the geologic model above (Table 2.1) we generate the acoustic impedance, reflection coefficient, and seismic seismogram for different frequencies. One of the purposes is to find the optimum frequency to distinguish all reflectors in the seismogram.

There are two kinds of reflection coefficients. They can be acoustic or elastic, and they can be normal or angular. Acoustic reflection coefficient involves P-wave only where elastic reflection coefficient includes both P and S waves. Normal reflection coefficient is the same as zero-offset which is a special case of the angular reflection coefficient. In this study, we used the acoustic reflection coefficient at zero-offset which is defined as the following:

$$R_o = \frac{I_2 - I_1}{I_2 + I_1}, \quad I = \rho V_p \quad (2.1)$$

where

R_o = Reflection coefficient

I = P-wave impedance

ρ = Mass density

The zero-offset seismic reflection coefficient function above is a function of geologic factors that change the seismic velocity and density. The geologic factors that can affect the reservoir velocity and density include lithology, gas, porosity, and clay content. Gas has lower velocity and density compared to oil and water, existence of

which in reservoir rocks increases reflection coefficient magnitude causing what is known as “bright spot”. However, not all bright spots are gas effect. Clay is important because of its effect on reducing reservoir permeability but it is more common in sandstone reservoirs than in carbonates.

The convolutional model can be expressed as the following:

$$T(t) = R(t) * w(t) + n(t) \quad (2.2)$$

where

$T(t)$ = seismic trace as a function of time

$R(t)$ = reflection coefficient

$w(t)$ = wavelet

$n(t)$ = noise

* = convolution

The acoustic impedance for each layer is calculated by multiplying the density and the velocity of that layer. Using the reflection coefficient function we can calculate the reflection coefficient series by placing each (R_o) at its correct time. The wavelet used in this study is the Ricker wavelet. The convolutional model in Eq. 2.2 is used to generate a synthetic seismic trace. Intuitively it means that one hangs the wavelet $w(t)$ at each spike location in the reflection coefficient series multiplied by the reflection coefficient at this location. All the wavelets are then added up to create the seismic trace. Doing the same for each trace gives us the seismic seismogram (Liner, 1999).

Results

The limit of seismic resolution based on bed thickness is equal to one quarter of wavelength. If the bed thickness is less than this limit, the top and bottom reflections are combined as one event. If the bed thickness is thicker than $\lambda/4$ the top and bottom reflections are distinguished as individual peaks. However, In order to distinguish the effects of different carbonate rock types on travel time, amplitude and waveform, we in this study further require that seismic signature of each rock type is separated completely from the signatures of the other rock types without any interference between each other. Therefore, the limit of the vertical seismic resolution used in this study is required to be half the seismic wavelength, considering two-way travel time.

Using the following equation we can calculate the bed thickness as a function of velocity and frequency. We can change the function to find the frequency as a function of velocity and bed thickness.

$$d = \frac{\lambda}{2} = \frac{v}{2f} \quad \Rightarrow \quad f = \frac{v}{2d} \quad (2.3)$$

where

λ = seismic wavelength

d = bed thickness

v = seismic interval velocity

f = dominant frequency

To find the optimum thickness using 25Hz frequency for the geologic model described in Table 2.1, the bed thickness of each layer should be 80 meters thick. However the thinnest layer is 5 meters thick in the model. Based on the function (2.3) above, the frequency required to view this thin layer should not be less than 400Hz, which is unrealistic.

Figures 2.2, 2.3, and 2.4 show the results of the convolutional model where the first columns on the left is the acoustic impedance, the column in the middle is the reflection coefficient, and the one on the right is the seismogram based on 25, 50, and 100Hz respectively. The top of the reservoir, which is the seal, and the fractured layer below have opposite polarities. From the seismograms we cannot distinguish the fractured layer because the layers is below the limit of vertical seismic resolution.

With 25Hz frequency we are only able to see the top and the bottom reflections of the reservoir (Figure 2.2). By increasing the frequency we are able to distinguish the top interface of different layers of the different carbonate rock types within the reservoir such as the fractured, grainstone, and wackestone layers. Using 100Hz we start seeing the top of the wackestone layer. All reflectors are visible in the seismic seismogram when a dominant frequency of 400Hz is used.

Increasing the frequency to 50Hz, we see a reflection right before the bottom of the reservoir (Figure 2.3). However, it is not clear from which interface exactly it comes because of the interference from other reflectors.

Using a dominant frequency up to 100Hz we can see clearly the reflection from the wackestone/grainstone interface (Figure 2.4). However, we are still unable to see the reflections from the top interface of the fractured and the grainstone layers because their bed thicknesses are below the limit of the vertical seismic resolution.

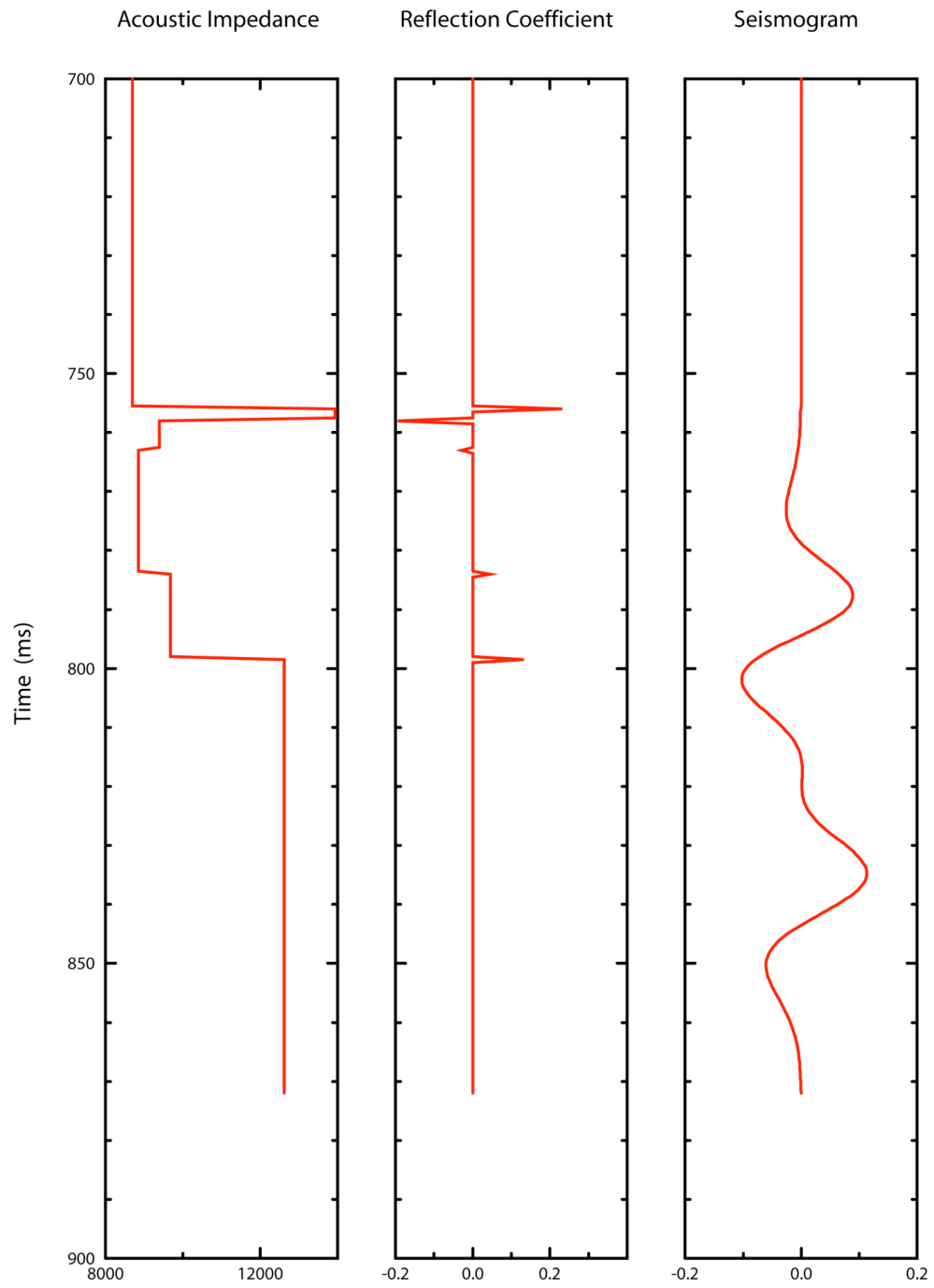


Figure 2.2. Convolutional modeling with 25Hz dominant frequency.

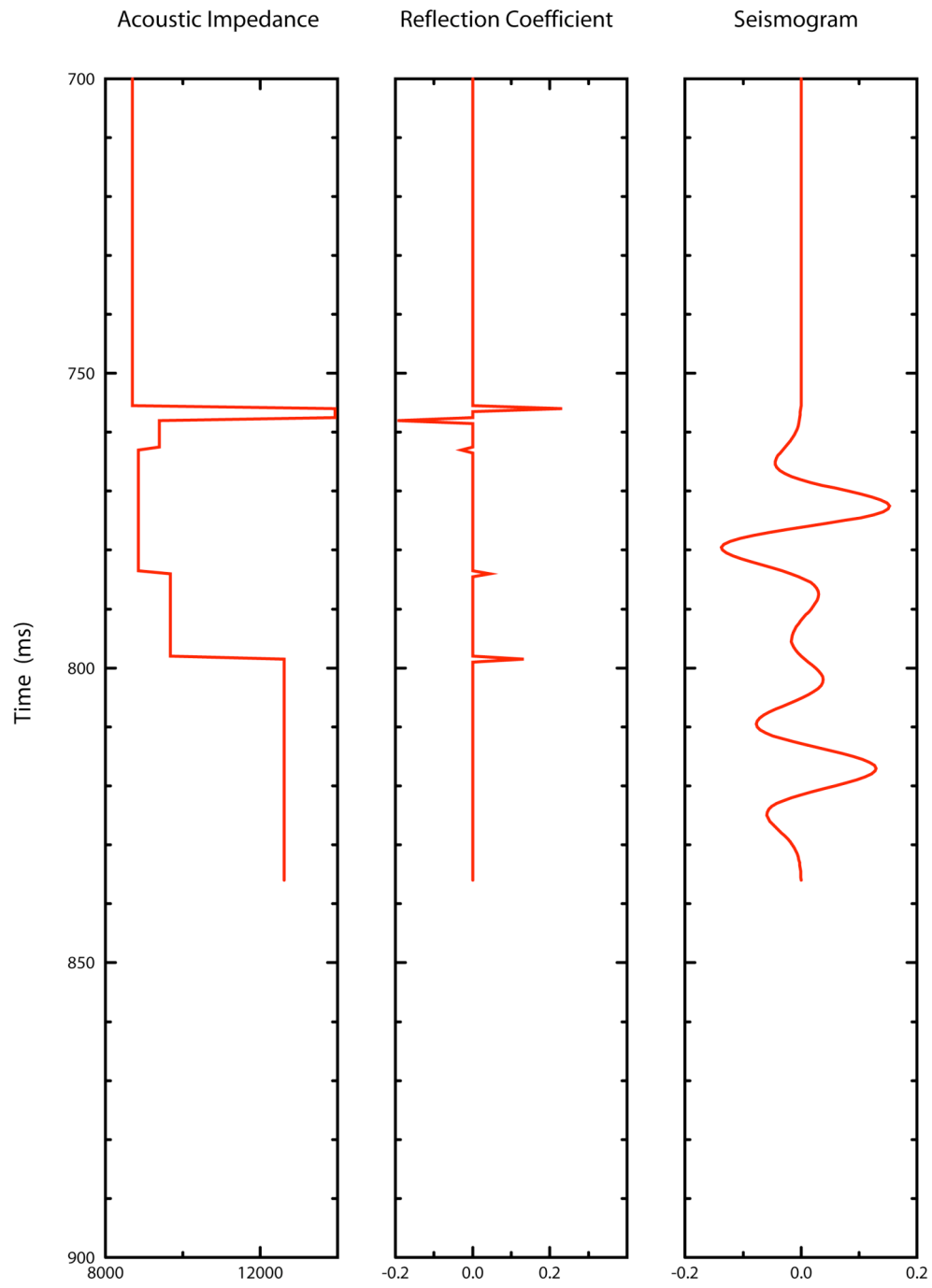


Figure 2.3. Convolutional modeling with 50Hz dominant frequency.

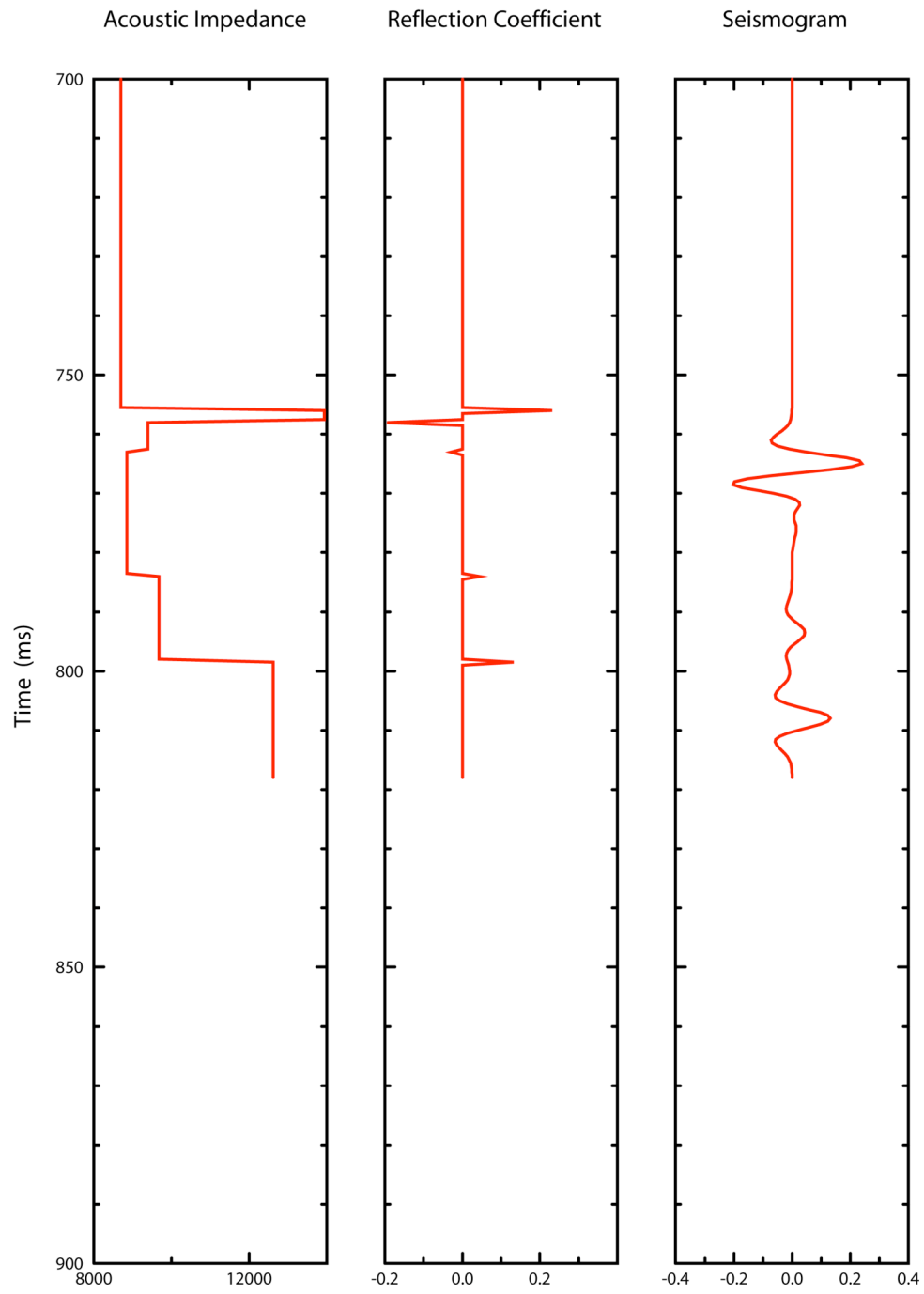


Figure 2.4. Convolutional modeling with 100Hz dominant frequency.

In terms of seismic reflection strength, the seal/overburden and the dense limestone/wackestone interfaces have the strongest amplitude. The interface between the grainstone and the fractured layer is about 7 times weaker than the seal and the overlying layers amplitude, and the interface between the wackestone and the grainstone is about 6 times weaker than the seal/overburden interface. However, the seismic reflection amplitude of the carbonate rock types within the reservoir is strong enough to be detectable in the seismic data.

Based on the definition of seismic vertical resolution we use in this study ($\lambda/2$), the optimum thickness for a dominant frequency of 25Hz is 80 meters. For the 50Hz, the bed thickness is 40 meters. Finally for the 100Hz the layers should be at least 20 meters thick.

To be able to separate the seismic signature of the top interface of the fractured layer completely from the signatures of other layers, the fractured layer thickness should not be less than the optimum thickness for the frequency used. Figures 2.5, 2.6, and 2.7 show the results of the convolutional model where all the layers thicknesses are set equal to the optimum thickness corresponding to dominant frequencies of 25, 50, and 100Hz respectively.

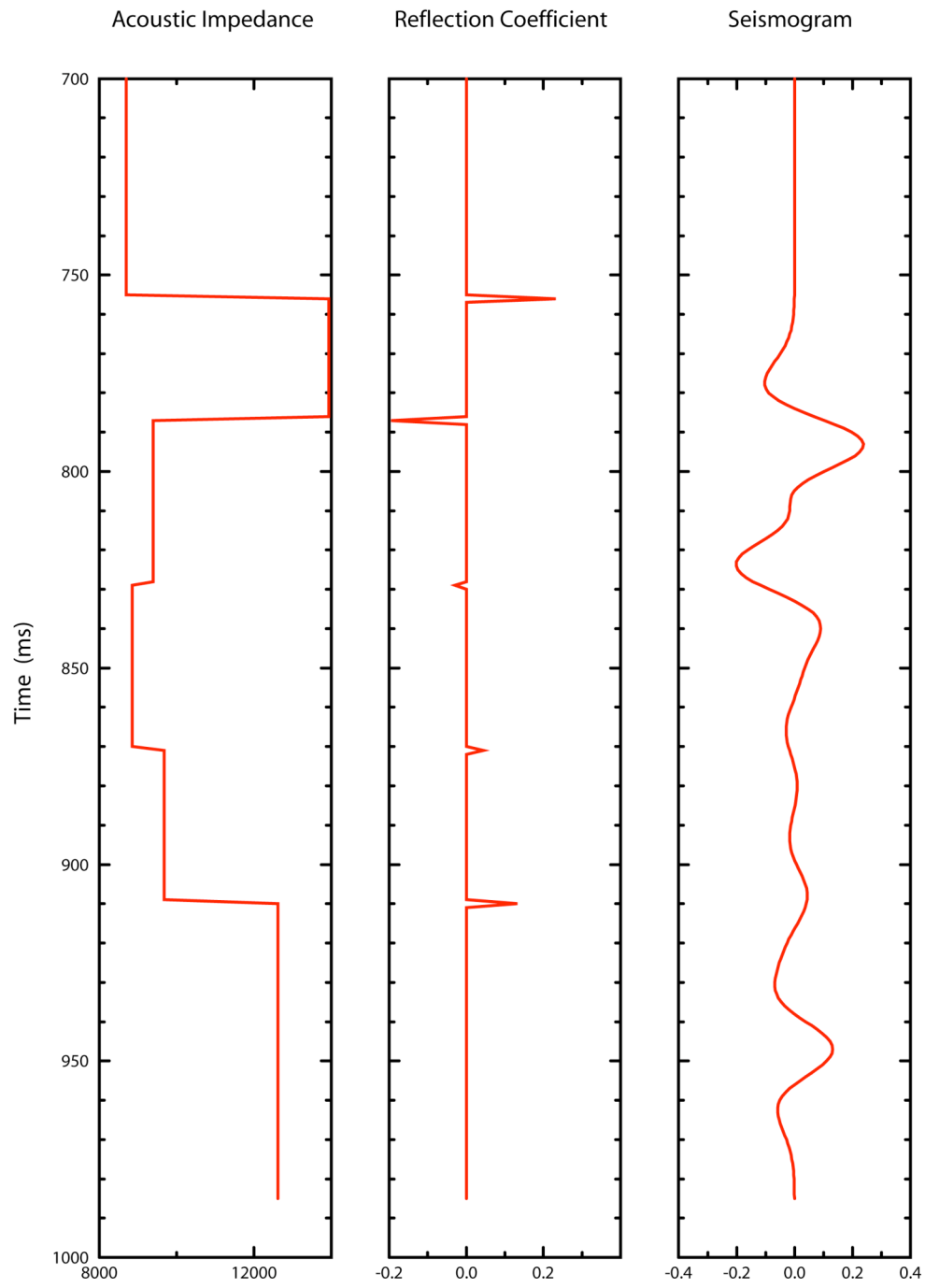


Figure 2.5. Convolutional modeling using equal thickness for the layers with 25Hz dominant frequency.

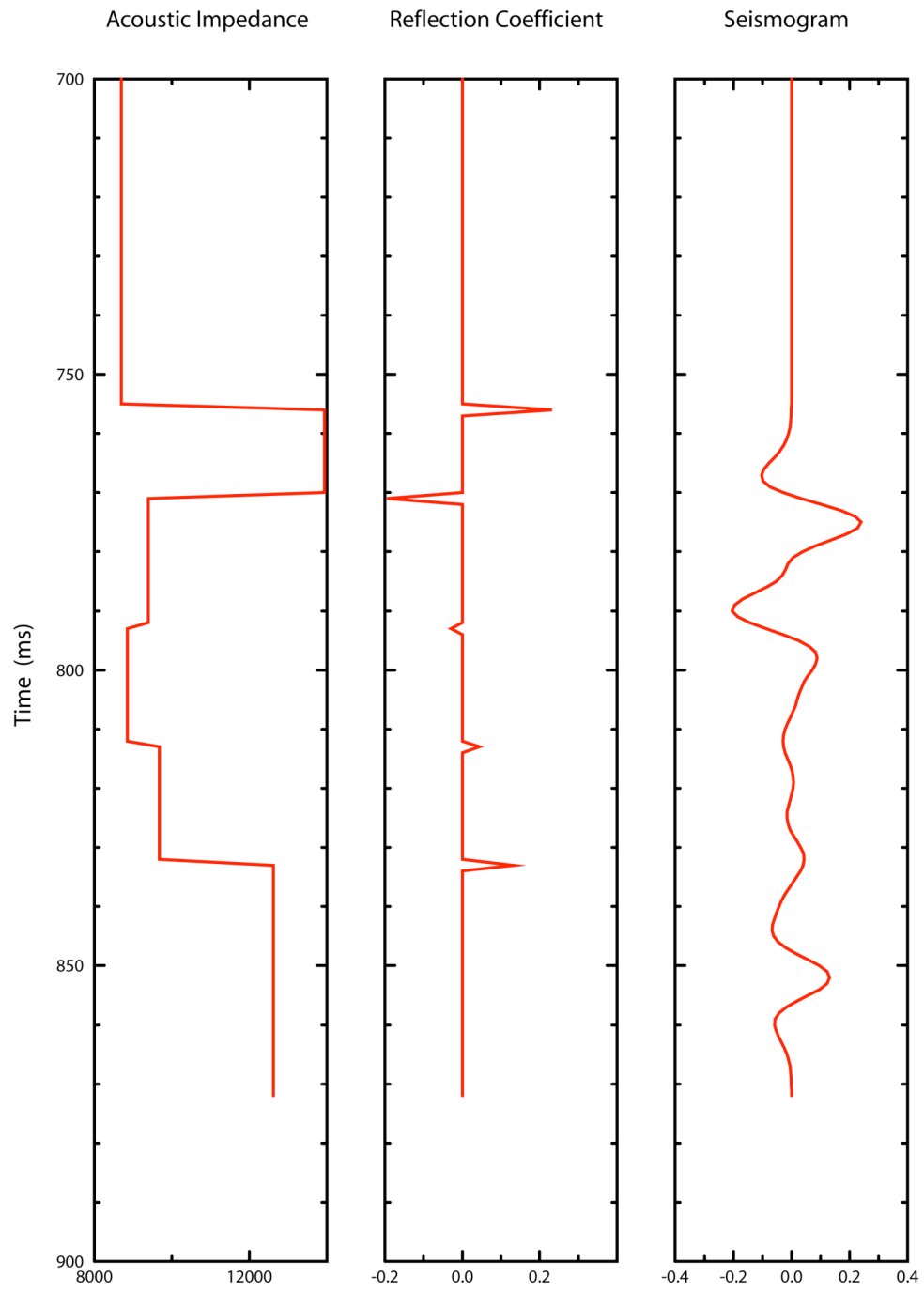


Figure 2.6. Convolutional modeling using equal thickness for the layers with 50Hz dominant frequency.

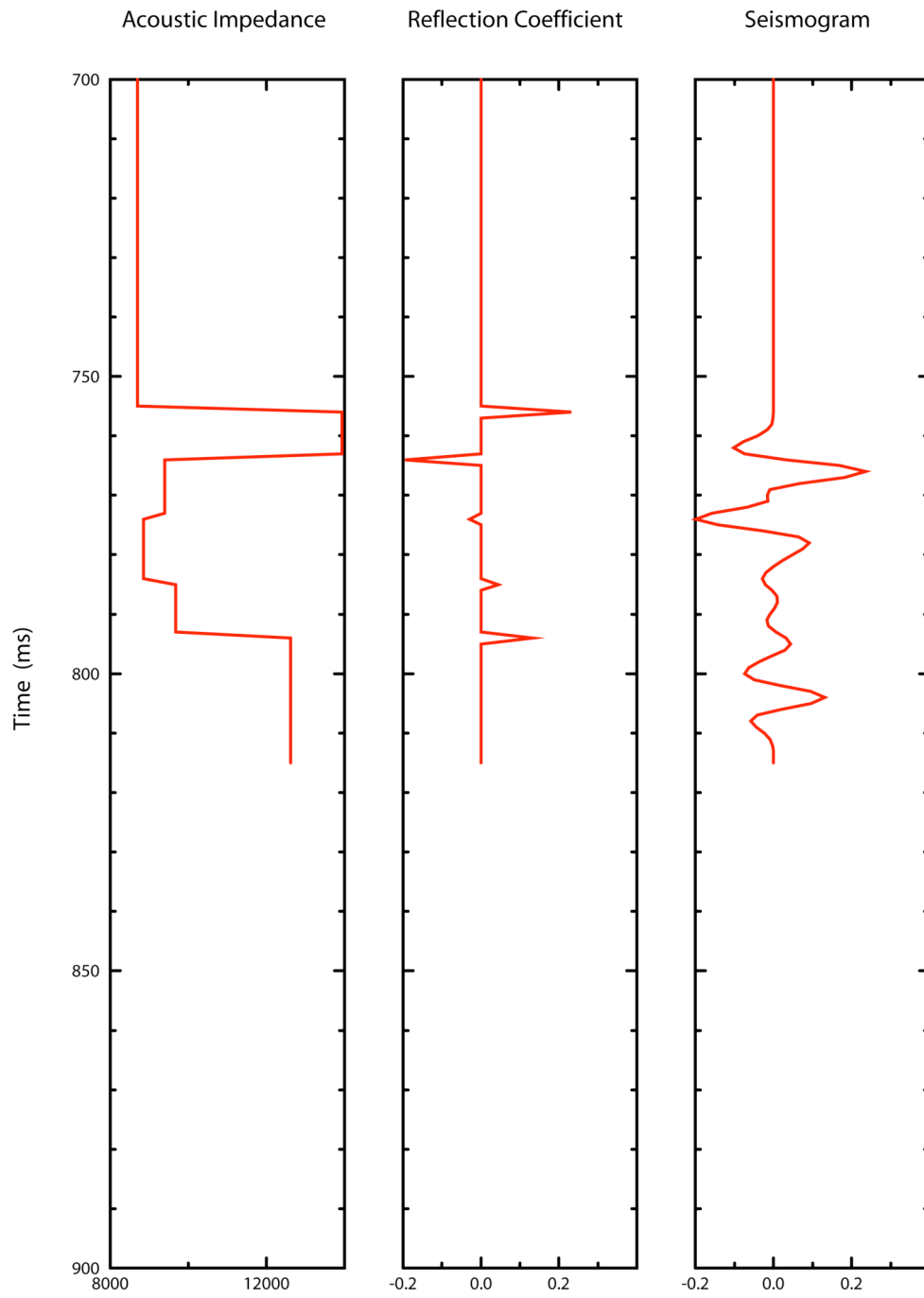


Figure 2.7. Convolutional modeling using equal thickness for the layers with 100Hz dominant frequency.

Conclusion

It is possible to predict some carbonate rock types using the convolutional model such as the grainstone/wackestone interface. However, high seismic resolution is needed to distinguish the thin layer. Using this simple model we are able to identify the optimum seismic resolution and thickness for the geologic model used in this study.

- The optimum frequency to visualize all the layers in the geologic model used in this study (Table 2.1) is 400Hz, which is unrealistic in field application.
- The optimum thickness to be visible in the seismic seismogram is:
 - 80 meters using a dominant frequency of 25Hz
 - 40 meters using a dominant frequency of 50Hz
 - 20 meters using a dominant frequency of 100Hz

In the geologic model studied in this thesis, the acoustic impedance of the fractured layer is lower than the seal above by 38% so that the interface between the two has negative reflection coefficient. The seismic reflection amplitude of the fractured/seal interface is weaker than the seal/overburden interface by 4%.

The acoustic impedance of the grainstone is lower than the fractured layer above by 6%, so that the reflection coefficient of the grainstone/fractured interface is negative. The seismic reflection amplitude of the grainstone/fractured interface is 17% of that from the fractured/seal interface.

The acoustic impedance of the wackestone layer is higher than the grainstone layer above by 8% so that the wackestone/grainstone interface has a positive reflection coefficient. The seismic reflection strength of the wackestone/grainstone interface is 23% of that from the fractured/seal interface.

The dense limestone layer at the bottom of the reservoir has higher acoustic impedance than the wackestone layer above by 26%. The seismic reflection strength of the dense limestone/wackestone interface is 69% higher than that from the fractured/seal interface.

The fractured layer in the geologic model used is not visible because the bed thickness is below conventional seismic resolution. Other methods should be used to detect thin layers away from the well such as seismic attribute analysis, 4-D time-lapse or amplitude variation with offset (AVO) analysis.

CHAPTER III

SEISMIC MODELING OF CARBONATE ROCK TYPES USING FINITE DIFFERENCE MODEL

Introduction

In Chapter II we generated the synthetic seismic data using the convolutional model based on the geologic model we constructed. This would represent the seismic data at the well location. In this chapter, we generate synthetic seismic data using the finite difference model (FDM) based on the same geologic model as used in the previous chapter. The one-dimensional geological model is extended horizontally to obtain a two-dimensional layered geological model. This will generate seismic data away from the well. Matching the results from the convolutional model and the zero-offset trace from the finite difference model will enable us to predict the different carbonate rock types in between wells. Amplitude variation with offset (AVO) could be also used to determine rock types.

Solving the differential equations that describes seismic wave propagation is ideal to simulate seismic surveys. Finite difference model is considered as one of the most accurate methods to describe wave propagation (Ikelle and Amundsen, 2005). Providing the right model parameters for FDM will result in better results when solving

the wave equation. The wave equations, in time domain, are to be solved time step by time step recursively

Method

A 2-D geological model is extended horizontally from the 1-dimensional geologic model used in Chapter I, which is based on a producing carbonate field in the Middle East. First we describe the geologic model by setting the parameters for the finite difference grid by discretizing time and space domains. The boundary conditions are set to be absorbing to eliminate the ghost reflection generated from the free surface and the artificial reflections from the left, right and bottom boundaries of the model. Different values for dominant frequency will be used in this study to examine the optimum frequency to resolve the carbonate rock types. Only the P-waves are used in this model in order to be compared with the convolutional model.

The spatial sampling intervals in both horizontal and vertical directions are $\Delta x = \Delta z = 2.5\text{m}$. The grid size (x,z) is 2000x300. The grid size in the horizontal direction is nearly three times of the vertical direction in order to observe the AVO effect in the far offset. The temporal sampling rate used is $\Delta t = 0.25\text{ms}$. The discretized wave equations are given in Ikelle and Amundsen (2005).

In order to interpret the FDM results, I summarize the basic features of wave propagation using ray theory. Seismic waves travel through earth layers and reflects

back up to the receivers. The recorded amplitude is approximated by the following function:

$$A = \frac{SD_S D_R R}{G} \prod_j T_j e^{\alpha l_j} \quad (3.1)$$

where

A	= received amplitude
S	= source amplitude
D_S, D_R	= source and receiver directivities
R, T_j	= reflection and transmission coefficients
G	= geometrical spreading function
Π	= product symbol
α	= attenuation factor
l_j	= raypath length
j	= counter for each layer traversed by the ray

As the waves travel through the earth, depending on array, coupling, and source type the take off angle is associated with some amplitude factor. As it propagates, the traveling wave undergoes amplitude decay due to geometric spreading. There is also amplitude loss due to conversion of energy to heat and transmission loss, which occurs whenever the waves go through an interface. The amplitude depends on the angular reflection coefficient, which is a function of the incident angle at which the wave hits the interface at the reflection point. As the waves reflect back to receivers more attenuation

and geometric spreading and transmission losses occur. The receivers measure the returned amplitude that depends on array directivity. However, the above equation ignores some factors such as:

- Source and receiver coupling
- Instruments performance
- Multiples, refraction, ground roll interference
- Random noise
- Data processing

The aim of data processing is to remove all these artifacts and keep reflections from the subsurface layers, but there are always some processing artifacts left in the data.

The post-stack seismic data does not have information about amplitude variation with offset because of the stacking process. AVO analysis is done on prestack data. In AVO analysis, the reflection coefficients depend upon the incidence angle. The angular acoustic reflection coefficient is:

$$R(\theta) = \frac{I_2 \cos \theta - I_1 \sqrt{1 - \left(\frac{v_2 \sin \theta}{v_1}\right)^2}}{I_2 \cos \theta + I_1 \sqrt{1 - \left(\frac{v_2 \sin \theta}{v_1}\right)^2}} \quad (3.2)$$

where

- θ = incidence angle
- I = acoustic impedance
- v = velocity

The square root in the angular reflection coefficient function means that the $R(\theta)$ can be also a complex number.

From the Snell's law the critical angle is:

$$\theta_C = \sin^{-1}(v_1/v_2) \quad ; \quad v_1 < v_2 \quad (3.3)$$

Substituting the θ_C into the square root term in the angular reflection coefficient we get the following formula:

$$\sqrt{1 - \left(\frac{v_2 \sin \theta_C}{v_1}\right)^2} = \sqrt{1 - \left(\frac{v_2(v_1/v_2)}{v_1}\right)^2} = 0 \quad (3.4)$$

When the incident angle is equal to the critical angle, the value under the square root is equal to zero. When it is less than the critical angle, it is positive. And when it is bigger than the critical angle, it is negative, which is known as postcritical reflection.

When the elastic P-wave hits an interface at an angle there will be four waves generated. There will be reflected P-wave, reflected S-wave, transmitted P-wave, and transmitted S-wave. AVO studies show a direct relationship between amplitude and offset in gas reservoirs. While, non-gas reservoirs or reflectors show little increase in amplitude with increasing offset (Liner, 1999).

Results

1. Comparison with Convolutional Model

The similar methodology in the convolutional model is used here. Starting with center frequency equal to 25Hz, 50Hz, and 100Hz we generate synthetic seismic shot records using the finite difference model.

From the synthetic record of FDM modeling with a dominate frequency of 25Hz we can see two reflections only coming from the top and the bottom of the reservoir interfaces (Figure 3.1). As reflections are relatively weak compared with direct waves, reflections can be better seen when direct waves are removed as shown in Figure 3.1.

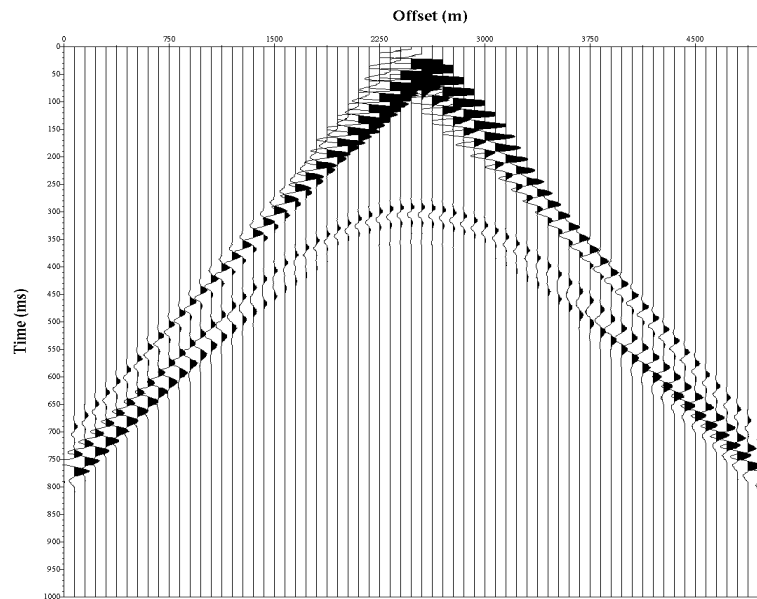


Figure 3.1. Shot records using FDM. (Top) Shot record using 25Hz based the original geologic model. (Bottom) the top part of the shot record is removed to reduce the effect of direct waves.

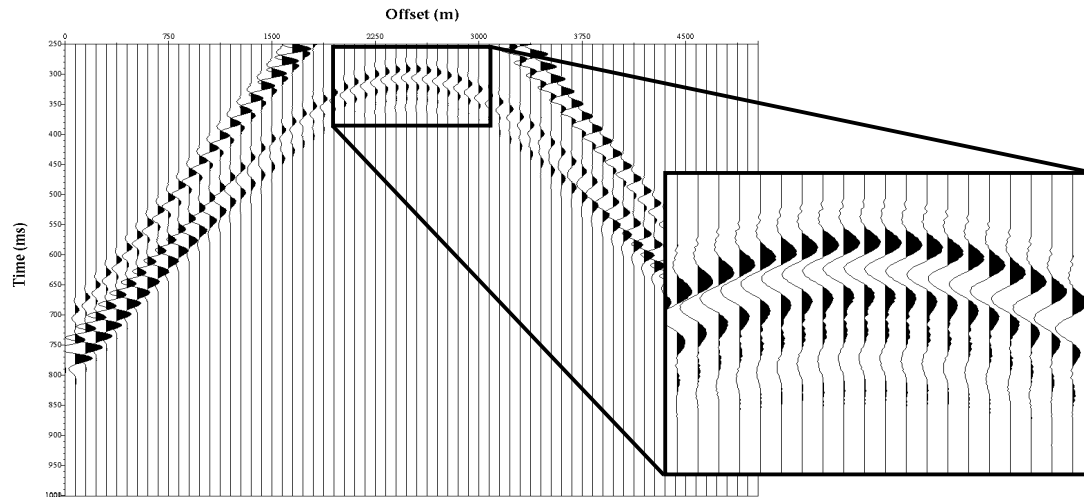


Figure 3.1. Continued.

More reflections show up as we increase the frequency to 50Hz. But reflections are still interfering with each other (Figure 3.2). As we increase the frequency to 100Hz we are able to see all the reflections from the different interfaces within the carbonate reservoir (Figure 3.3). However, these reflections are interfered with each other due to the limitation of the vertical seismic resolution.

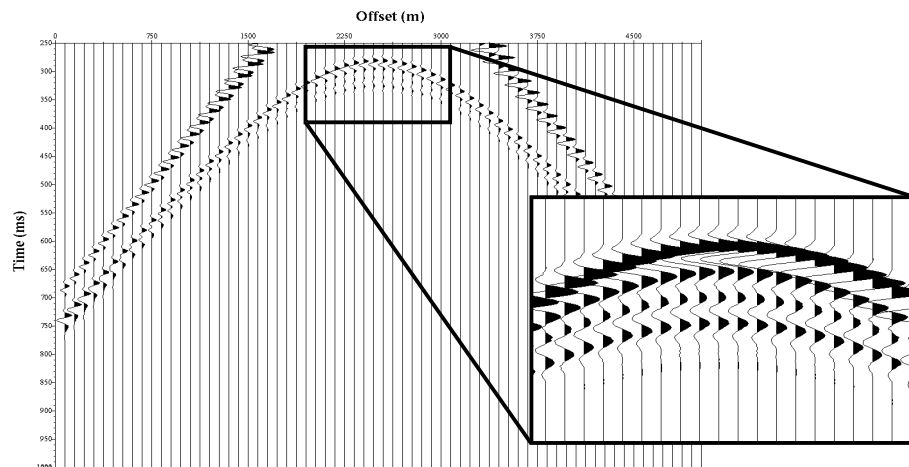


Figure 3.2. Shot record using 50Hz based the original geologic model.

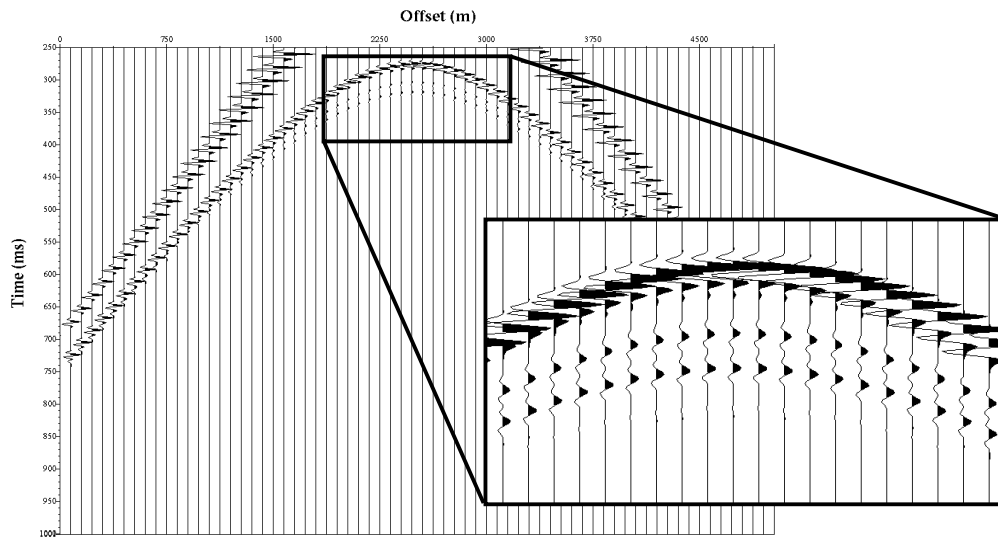


Figure 3.3. Shot record using 100Hz based the original geologic model.

The seismic signature at the well location from the convolutional model can be compared with the seismic signature from the finite difference model. This comparison would enable us to predict the different rock types away from the well in field applications. The figures below (Figures 3.4-3.6) show comparisons between the results of the convolutional model and those of finite difference model at different frequencies. They agree with each other very well.

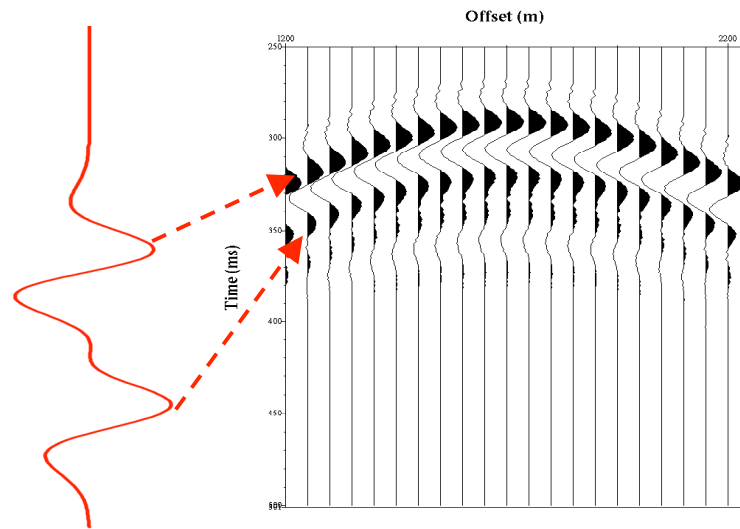


Figure 3.4. Comparison between the seismic signatures from convolutional model and finite difference model using 25Hz center frequency.

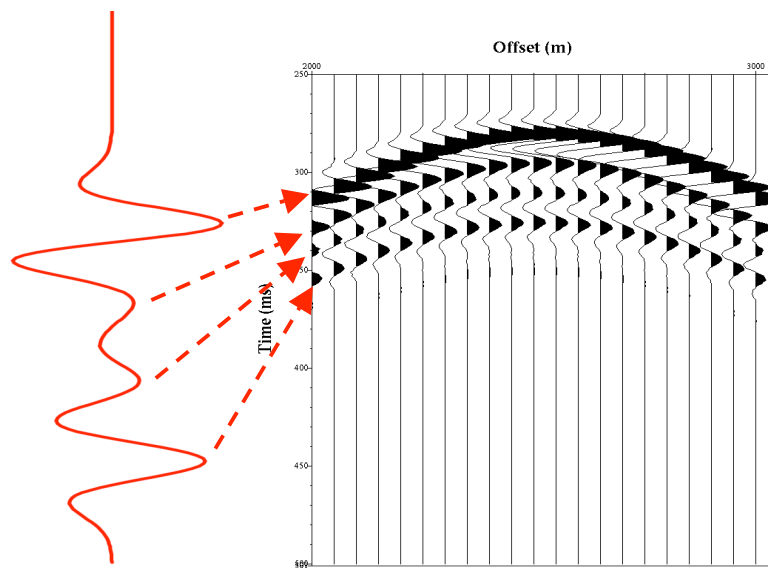


Figure 3.5. Comparison between the seismic signatures from convolutional model and finite difference model using 50Hz center frequency.

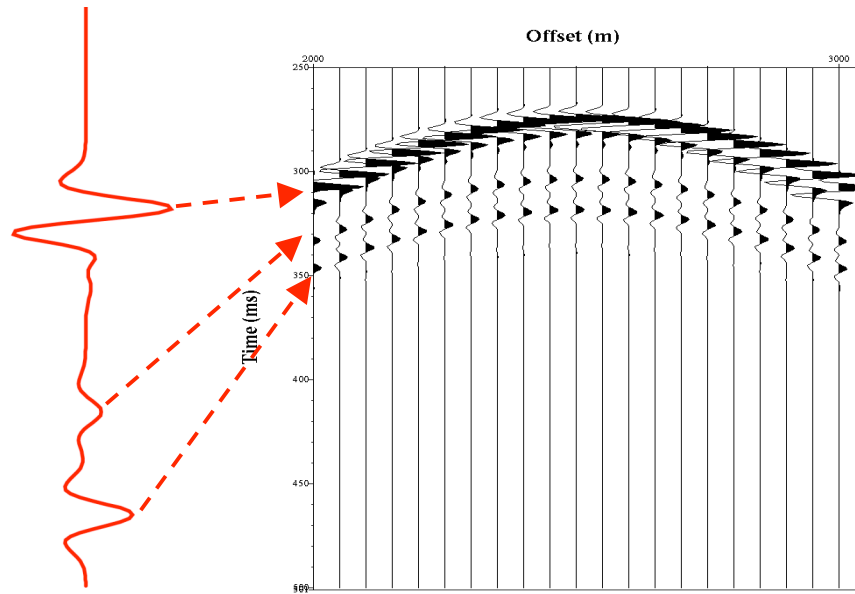


Figure 3.6. Comparison between the seismic signatures from convolutional model and finite difference model using 100Hz center frequency.

2. AVO signatures of carbonate rock types

For an interface between two different rock types, the reflection coefficient changes with incidence angle. Therefore, the reflection amplitude from that interface changes with offset. This knowledge, termed as amplitude variation with offset (AVO), has been used in the industry since 1982 when Ostrander showed how gas could cause amplitude change with offset in shot gathers (Ostrander, 1982; Chopra and Castagna, 2007).

The rock properties for the geologic model used in this study shown in Table 2.1 document very useful information, which can help understanding the seismic signatures of the different, carbonate rock types. The wackestone layer has lower seismic velocity than the dense limestone layer below. Therefore, it is expected to observe strong

amplitude change from the wackestone/grainstone interface with offset at the critical angle due to strong refracted seismic wave energy. Because the reflections from the top interface of the wackestone and the grainstone layers are separated from reflections from other interfaces without any ambiguity, we can observe the amplitude change very clearly with offset. At the near offset we barely see any amplitude, but at the far offset we see big amplitude change. The seal has higher velocity than the layers above and below, and it is also expected to observe a strong amplitude change with offset near the critical angle for the interface between the seal and the layers above. However, we do not observe this amplitude change with offset. Instead, the amplitude stays the same with slight increase at the far offset (Figure 3.7). The reason is that reflections from the fractured/seal and grainstone/fractured layers interfaces below are interfering with the reflection of the seal/overlying interface.

Detailed AVO analysis can thus help understand the changes in reservoir quality caused by the different carbonate rock types. In this study we can predict the presence of the fractured layer in the reservoir, using AVO analysis as outlined above.

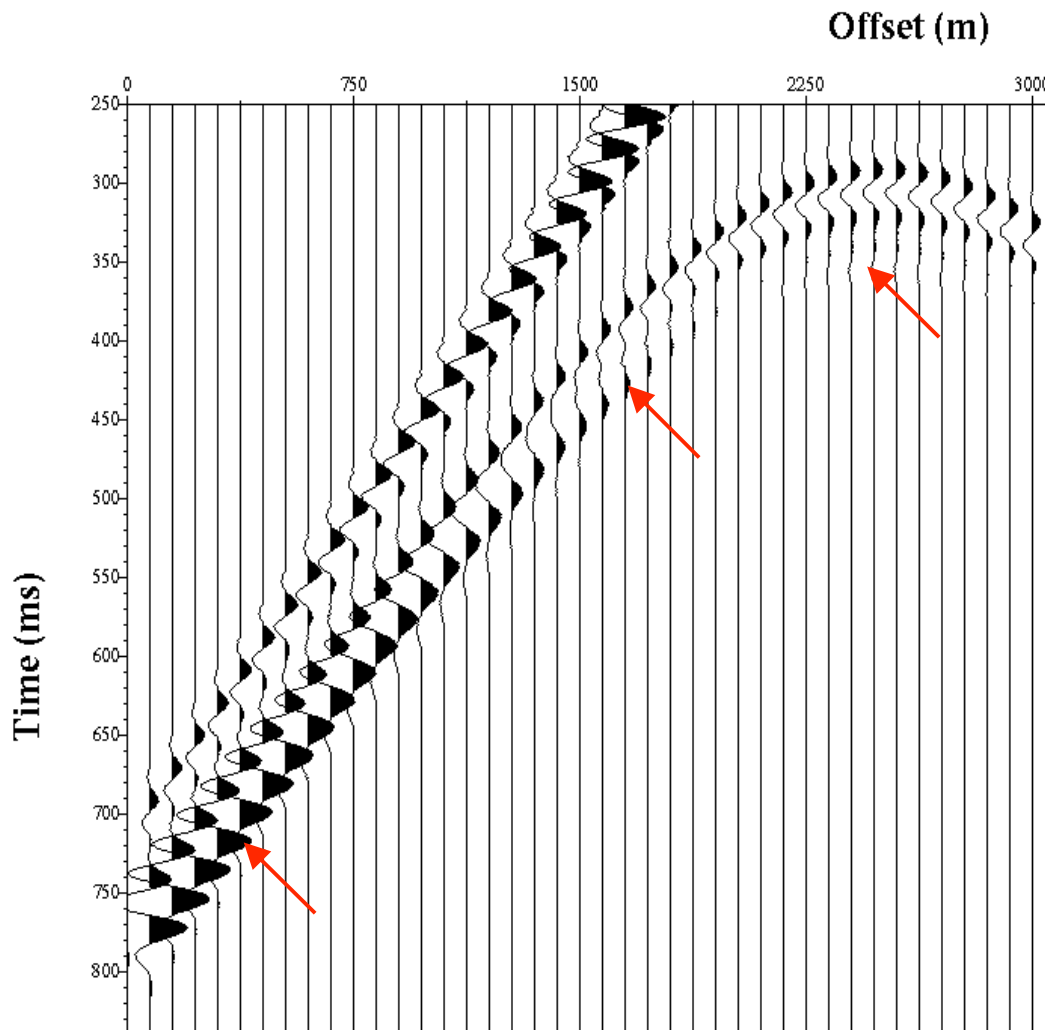


Figure 3.7. Shot record with 25 Hz dominant frequency. The arrows show amplitude increase with increasing offset.

Conclusion

Finite difference model can be used to predict the carbonate rock types by tying the results with the convolutional model. However, higher frequency seismic data is needed to detect the fractured thin layer.

The reflection from the seal top interface is expected to have weak amplitude at the near offset and gets stronger as offset increases. However, due to the interference of the fractured/seal and the grainstone/fractured interfaces below, the amplitude does not vary with offset but it stays nearly constant.

The amplitude from the dense limestone/wackestone interface is expected to show a normal AVO response because the layers above are thick enough for their amplitudes not to interfere with each other. The results, as expected, show that the amplitude from the dense limestone/wackestone interface is weak at the near offset and it increases as the offset increases.

Detailed amplitude variation with offset (AVO) analysis can help to detect anomalies in the reservoir due to changes in rock properties. Since we only used synthetic seismic data in this study, it is easier to understand the rock properties because there are fewer variables that can affect amplitude change.

CHAPTER IV

FLUID SUBSTITUTION

Introduction

The previous two chapters discussed the possibility of predicting the carbonate rock types by using their seismic signatures. The two techniques used are convolutional model and finite difference model. The results show that we can tie seismic signatures away from the well with the signatures at the well location. However, high seismic resolution must be acquired to distinguish all the carbonate layers within the reservoir, some of which can be thinner than the tuning thickness. Time-lapse analysis may help detect the fluid change in the reservoir that can be caused by super-k layers.

In this chapter, we use time-lapse technique to investigate the changes in the carbonate rock properties. Gassmann's equation for fluid substitution is used to predict the fluid properties after the oil is substituted by water in the fractured layer in the geologic model in Table 2.1. Following the calculation of rock properties after fluid substitution, the convolutional and finite difference models are applied on the new data.

Method

Modeling the fluid property change require a better understanding of fluid and reservoir property. First, the fractured layer is saturated with oil and the density, bulk modulus (bulk modulus = 1/compressibility), and shear modulus of both oil and the rock are calculated. Then the fractured rock layer is saturated with the new fluid, which in this study is water, and the new density and bulk modulus of rock are calculated. The shear modulus remains constant because it does not depend on pore fluid (Smith et al. 2003). After calculating the new density and bulk modulus we are able to calculate the primary and shear velocities after fluid substitution using the Gassmann's equation as the following:

$$\frac{1}{C - C_s} = \frac{1}{C_d - C_s} + \left(\frac{1}{C_f - C_s} \right) \frac{1}{\phi} \quad (4.1)$$

where

C = compressibility of the saturated rock

C_d = compressibility of the dry rock frame

C_s = compressibility of the matrix material

C_f = compressibility of the pore fluid

ϕ = porosity

Results

Gassmann's equation (4.1) is used only to calculate rock properties of the fractured layer in the geologic model used in this study to simulate fluid movement in this layer. Table 4.1 shows the rock properties of the fractured layer before and after fluid substitution.

Table 4.1. Rock properties for the fractured layer before and after fluid substitution.

	<i>Before</i>	<i>After</i>	<i>% Change</i>
<i>V_p (m/s)</i>	3785	3976	5.0
<i>V_s (m/s)</i>	1924	1927	0.2
<i>ρ (g/cc)</i>	2500	2493	-0.3
<i>AI</i>	9.46	9.91	4.8
<i>RC (top interface)</i>	-0.19	-0.17	-10.5
<i>RC (bottom interface)</i>	-0.03	-0.06	87

Figure 4.1 shows the result of convolutional model where the first column is the acoustic impedance, the second column is the reflection coefficient, and the last column is the seismogram. Note that in the geologic model used for the fluid substitution, the fractured layer is saturated with oil first. The central frequency used is 25Hz.

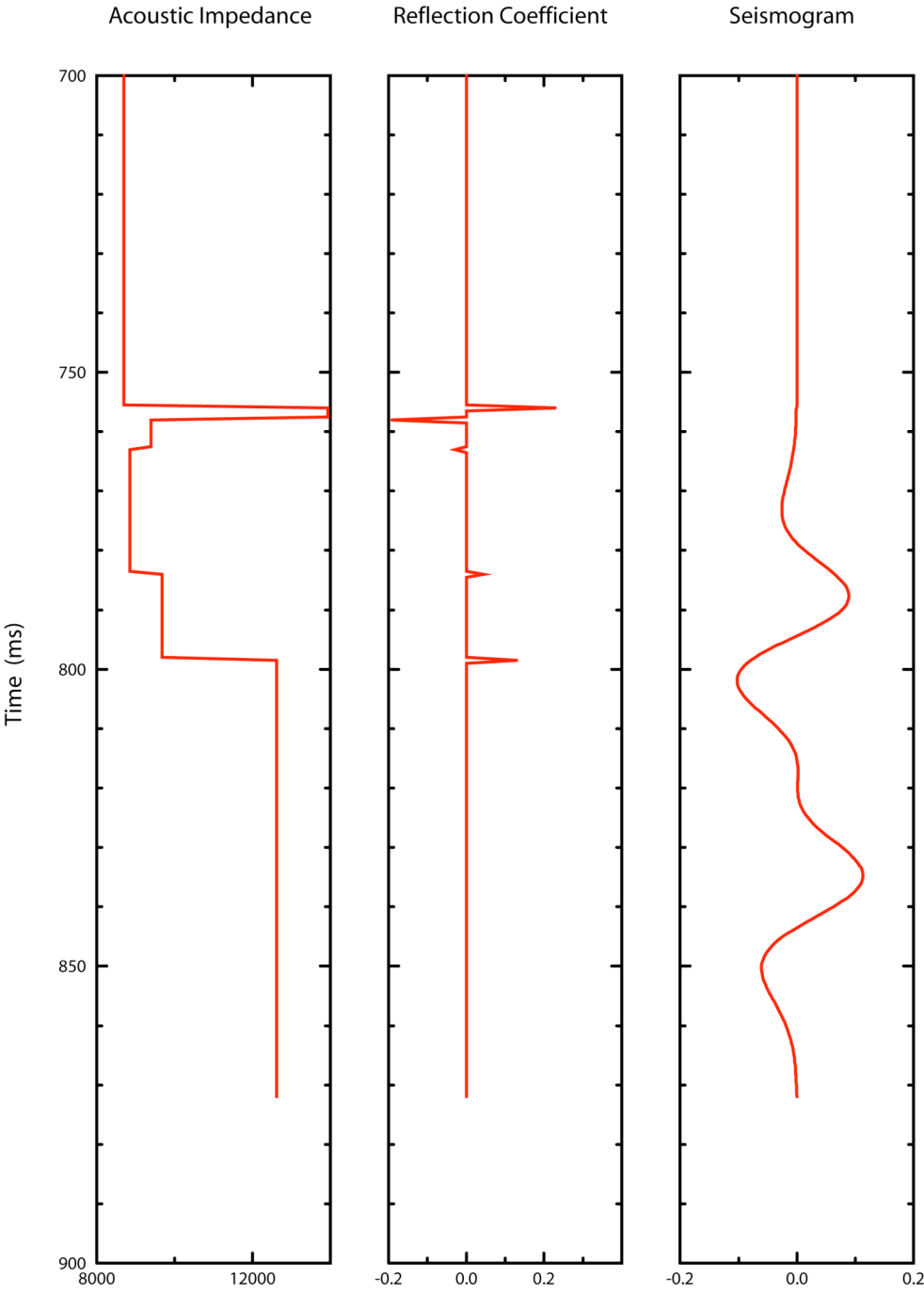


Figure 4.1. Results of convolutional model before fluid substitution.

The rock properties after substituting the oil with water in the fractured layer are then calculated. The convolutional model for the same geologic model with the new rock properties for the fractured layer is shown in Figure 4.2. Figure 4.3 shows the seismogram difference between the before and after fluid substitution.

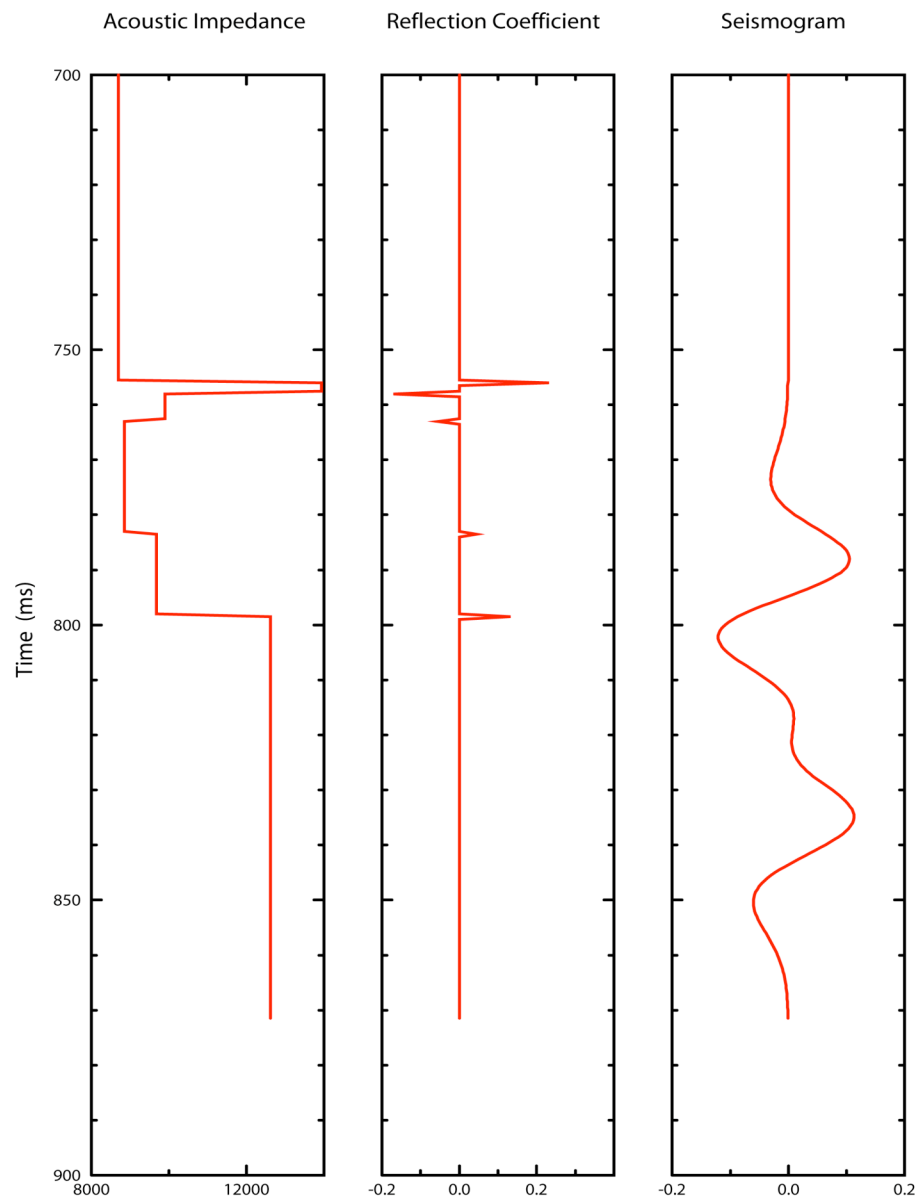


Figure 4.2. Results of convolutional model after fluid substitution.

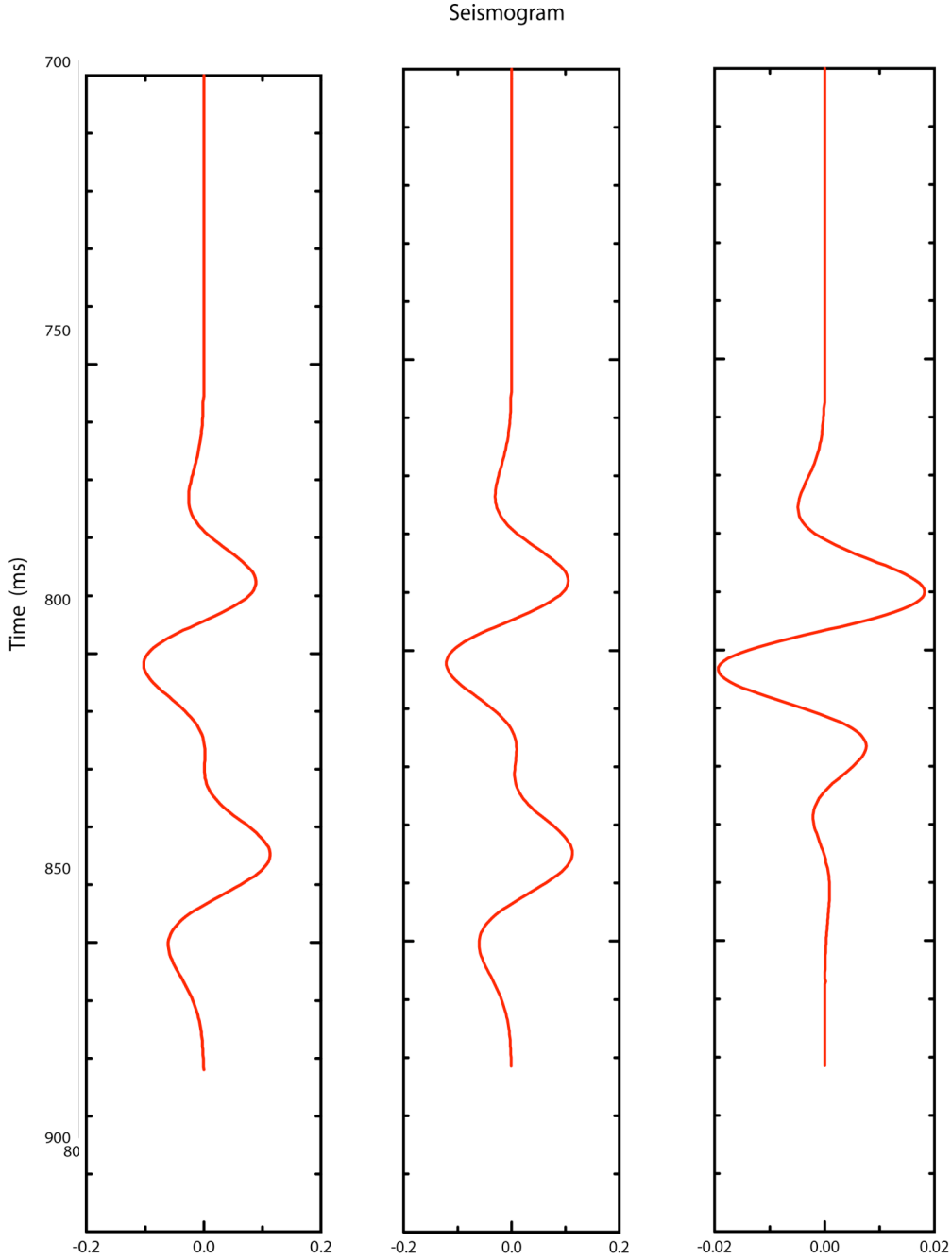


Figure 4.3. Fluid substitution result. (Left) seismogram before fluid substitution. (middle) seismogram after fluid substitution. (Right) seismogram difference between before and after fluid substitution.

We also apply the finite difference model for the same geologic model before and after fluid substitution using the same dominant frequency used in the convolutional model (25 Hz). Figure 4.4 shows a shot record for the geologic model before fluid substitution where the fractured layer is saturated with oil.

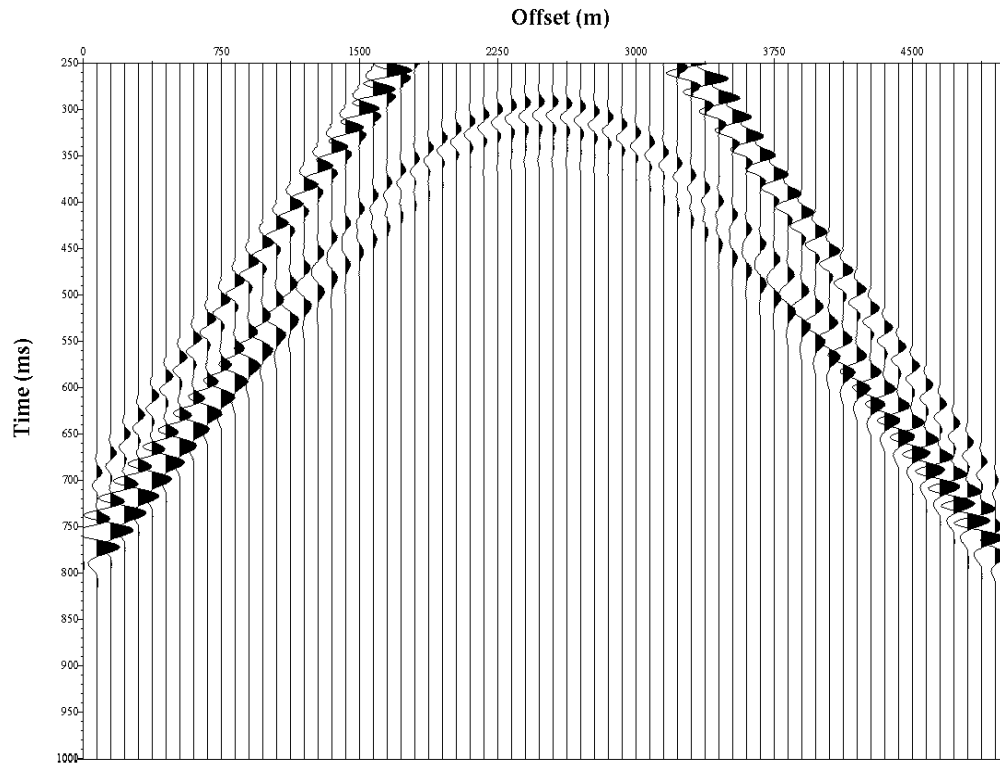


Figure 4.4. Finite difference model before fluid substitution with 25 Hz dominant frequency.

The shot record in Figure 4.5 is after fluid substitution where the oil in the fractured layer is substituted with water. The difference between the two shot records of before and after fluid substitution is shown in Figure 4.6. These results demonstrate that the thin layer cannot be detected either before or after the substitution. However, it can be well detected by the seismic difference.

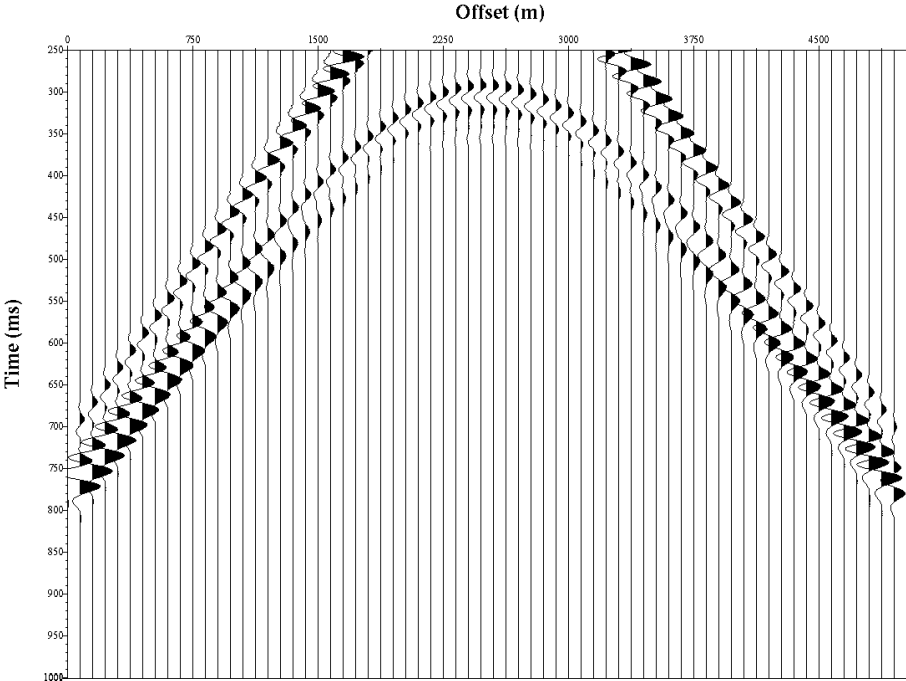


Figure 4.5. Finite difference model after fluid substitution with 25 Hz dominant frequency.

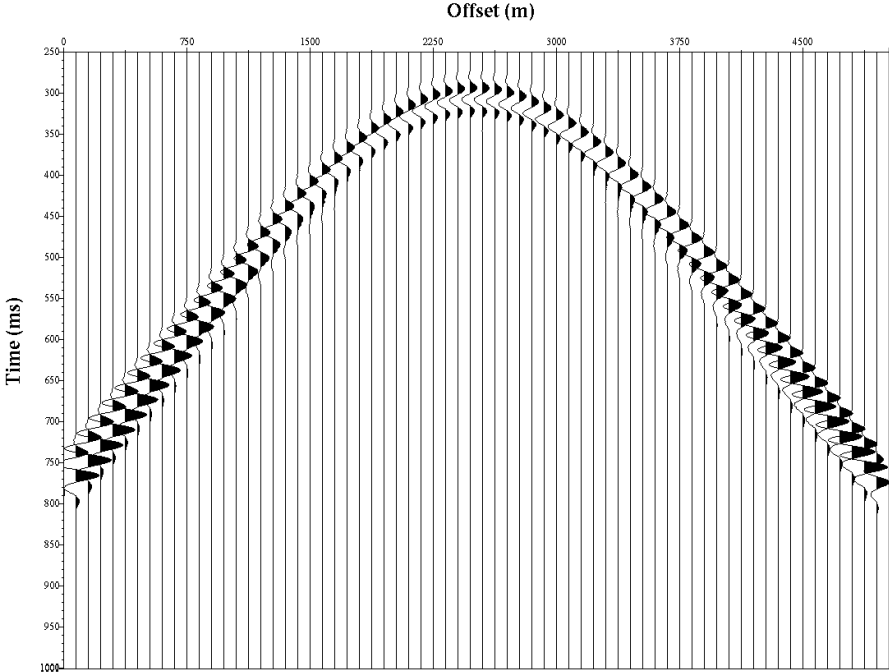


Figure 4.6. The difference between the before and after fluid substitution using the finite difference model.

Conclusion

Taking the difference of the convolutional seismograms before and after fluid substitution shows that it is possible to predict the signature change in fractured layer due to water replacing oil. Similar results achieved using the finite difference model.

The acoustic impedance of the fractured layer increased by 4.6% due to the velocity increase after water substituting the oil. Consequently the reflection coefficient of the top interface of the fractured layer with the overlaying seal has decreased by 11.8%. Changing the rock properties of the fractured layer will also change the reflection coefficient of the fractured/grainstone interface below. The results show that the reflection coefficient of the top grainstone/fractured interface has increased by 87%.

Replacing the oil in the fractured layer by water changes both the seismic waveform and the travel time. Since the seismic resolution is not high enough in the reservoir scale, it will be difficult to use time-lapse analysis when water is injected in other reservoir layers below the fractured layer. This is because the seismic changes due to water injection in the fractured layer will mask the seismic change in the layers below.

Fluid substitution method can help identifying the presence of the fractured super-k layers in carbonate reservoirs when water replaces oil in these layers. Other seismic attribute and AVO analysis should be used to minimize the uncertainty of the presence of fractured or super-k layers in a reservoir.

CHAPTER V

CONCLUSIONS

In this study I used the convolutional model, finite difference model, and fluid substitution method to study the seismic signature of carbonate rock types in the modeled reservoir. The seismic signatures of carbonate rock types help identifying the fractured super-k layer within the reservoir.

The seal/overburden interface has a positive reflection coefficient because the seal layer has high acoustic impedance than the layer above, and it has the strongest seismic reflection amplitude in the model we used. The fractured-carbonate/seal interface has a negative reflection coefficient, and the acoustic impedance of the fractured carbonate is lower than the seal above by 38%, and its seismic reflection amplitude is 4% weaker than the seal/overburden interface. The grainstone/fractured interface has a negative reflection coefficient. The acoustic impedance of the grainstone is lower by 6% than the fractured carbonate layer above. The seismic reflection amplitude of the grainstone/fractured interface is 17% of that from the fractured/seal interface above. The wackestone/grainstone interface has a positive reflection coefficient. The acoustic impedance of the wackestone layer is 8% higher than the grainstone layer above. The seismic reflection strength of the wackestone/grainstone interface is 23% of that from the fractured/seal interface. The acoustic impedance of the dense limestone layer is 26% higher than the wackestone layer above. And the seismic

reflection amplitude of the interface of the dense limestone/wackestone is 69% of that from the fractured/seal interface.

Seismic signature of carbonate rock layers within the seismic resolution modeled using FDM can be correlated to the signatures from the convolutional model. The reflections from the fractured/seal and the grainstone/fractured interfaces are mixed together with the reflection from the seal/overburden interface. Using AVO analysis we were able to predict the presence of the fractured layer, because of the non-AVO phenomena associated with seal and the fractured layer. The dense limestone/wackestone interface showed normal AVO response because there is no interference from other interfaces.

Thin fractured layer can also be identified using fluid substitution method. This method showed 5% increase in the acoustic impedance of the fractured layer, and 11% decrease in the reflection coefficient of the fractured/seal interface after fluid substitution.

The results show that it is possible to use these methods to help solving some of the typical problems in carbonate reservoirs. Synthetic seismic data is used in this study to quantify if these methods will be applicable in the industry. In order to apply the methods used in this study in field applications, high-resolution seismic data should be acquired.

REFERENCES

- Ahr, W. M., 2008, *Geology of carbonate reservoirs*: John Wiley & Sons Inc.
- Anselmetti, F. S., and Eberli, G.P., 1993, Controls on sonic velocity in carbonates: *Pure Applied. Geophysics*, **141**, 287-323
- Archie, G.E., 1952, Classification of carbonate reservoir rocks and petrophysical considerations: *AAPG Bull*, **36**, 278–298
- Bracco Gartner, G. L., W. Schlager, 1999, Discrimination between onlap and lithologic interfingering in seismic models of outcrops: *AAPG Bulletin*, **83**, 952-971.
- Chopra, S. and J. P. Castagna, 2007, Introduction to this special section-AVO: *The Leading Edge*, **26**, 1506.
- Crampin, S., and Peacock, S., 2008, A review of the current understanding of seismic shear-wave splitting in the Earth's crust and common fallacies in interpretation: *Wave Motion*, **45**, 675-722.
- Dasgupta, S. N., M. R. Hong, and I. A. Al-Jallal, 2001, Reservoir characterization of Permian Kuff-C carbonate in the supergiant Ghawar Field of Saudi Arabia: *The Leading Edge*, **20**, 706
- Davis, R. and J. Fontanilla, 1997, Lithology, lithofacies, and permeability estimation in Ghawar Arab-D reservoir: *SPE 37702*.
- Dunham, R. J., 1962, Classification of carbonate rocks according to depositional texture, in Ham, W.E., ed., *Classification of carbonate rocks: Memoir*, American Association of Petroleum Geologists, 108-121.

- Folk, R. L., 1959, Practical petrographic classification of limestones: AAPG Bull, **43**, 1-38
- Ikelle, L. T., and L. Amundsen, 2005, Introduction to petroleum seismology: Society of Exploration Geophysicists.
- Liner, C. L., 1999, Elements of 3-D seismology: PennWell.
- Liner, C. L., 2004, Elements of 3-D seismology: 2nd edition, PennWell.
- North, F. K., 1985. Petroleum geology. Allen & Unwin.
- Ostrander, W. J., 1982, Plane-wave reflection coefficients for gas sands at non-normal angles-of-incidence: Geophysics, **49**, 1637-1648
- Palaz, I., and K. J. Marfurt, 1997, Carbonate seismology: SEG Geophysical Developments Series, 6.
- Sayers, C. and R. Latimer, 2008, An introduction to this special section: Carbonates: The Leading Edge, **27**, 1010-1011.
- Schlumberger, 2007, Carbonate reservoirs,
<http://www.slb.com/media/services/solutions/reservoir/carbonate_reservoirs.pdf>
Accessed January 5,2009.
- Schlumberger, 2009, Dunham's classification of carbonate rocks,
<<http://www.glossary.oilfield.slb.com/DisplayImage.cfm?ID=24>> Accessed
September 29, 2009.
- Smith,T. M. , C. H. Sondergeld, and C. S. Rai, 2003, Gassmann fluid substitutions: A tutorial: Geophysics, **68**, 430-440.

- Sun, Y.F., 2004, Pore structure effect on elastic wave propagation in rocks: AVO modeling: *Journal of Geophysics and Engineering*, **1**, 268-276, doi: 10.1088/1742-2132/1/4/005.
- Wagner, P. D., 1997, Seismic signatures of carbonate diagenesis, in I. Palaz, and K. J. Marfurt, *Carbonate seismology: Society of Exploration Geophysicists*, 307-320.
- Wang, Z, 1997, Seismic properties of carbonate rocks, in I. Palaz, and K. J. Marfurt, *Carbonate seismology: Society of Exploration Geophysicists*, 29-52.
- Wolfgang S., 1999, Sequence stratigraphy of carbonate rocks: *The Leading Edge*, **18**, no. 8, 906.

VITA

Name: Badr H. Jan

Address: Aramco Services Company
Career Development Department
9009 West Loop South
Houston, TX 77096

Email Address: badr.jan@aramco.com

Education: B.S., Geophysics, University of Tulsa, 2003